PLASMA PROCESSES OF CUTTING AND WELDING

FEBRUARY 1976

Report Documentation Page

Form Approved
OMB No. 0704-0188

1. REPORT DATE	2. REPORT TYPE	3. DATES COVERED
1971	**N/A**	**-**

4. TITLE AND SUBTITLE	5a. CONTRACT NUMBER
Plasma Processes of Cutting and Welding	5b. GRANT NUMBER
	5c. PROGRAM ELEMENT NUMBER
6. AUTHOR(S)	5d. PROJECT NUMBER
	5e. TASK NUMBER
	5f. WORK UNIT NUMBER
7. PERFORMING ORGANIZATION NAME(S) AND ADDRESS(ES) **Naval Surface Warfare Center CD Code 2230- Design Integration Tools Building 192, Room 138 9500 MacArthur Blvd Bethesda, MD 20817-5000**	8. PERFORMING ORGANIZATION REPORT NUMBER
9. SPONSORING/MONITORING AGENCY NAME(S) AND ADDRESS(ES)	10. SPONSOR/MONITOR'S ACRONYM(S)
	11. SPONSOR/MONITOR'S REPORT NUMBER(S)

12. DISTRIBUTION/AVAILABILITY STATEMENT
Approved for public release, distribution unlimited

13. SUPPLEMENTARY NOTES

14. ABSTRACT

15. SUBJECT TERMS

16. SECURITY CLASSIFICATION OF:			17. LIMITATION OF ABSTRACT	18. NUMBER OF PAGES	19a. NAME OF RESPONSIBLE PERSON
a. REPORT	b. ABSTRACT	c. THIS PAGE			
unclassified	**unclassified**	**unclassified**	**SAR**	**82**	

Standard Form 298 (Rev. 8-98)
Prescribed by ANSI Std Z39-18

FOREWORD

The purpose of this report is to present the results of one of the research and development programs which was initiated by the members of the Ship Production Committee of The Society of Naval Architects and Marine Engineers and financed largely by government funds through a cost sharing contract between the U. S. Maritime Administration and Bethlehem Steel Corporation. The effort of this project was directed to the development of improved methods and hardware applicable to shipyard welding in the U. S. shipyards.

Mr. W. C. Brayton, Bethlehem Steel Corporation was the Program Manager, Mr. J. A. Hogan, Union Carbide Corporation directed the development work at Florence, South Carolina with assistance from Messrs. J. B. Lewis and Alexander Jordan.

Special acknowledgement is made to the members of Welding Panel SP-7 of the SNAME Ship Production Committee who served as technical advisors in the preparation of inquiries and evaluation of sub-contract proposals.

SUMMARY

This report analyzes the latest developments in plasma arc cutting, welding and shape cutting machines with emphasis on their application in the shipbuilding industry. Plasma welding is found to have advantages over other welding processes for only a few shipyard requirements. Plasma cutting, on the other hand, is shown to be ideally suited for the productivity, quality and operating cost necessary in modern shipbuilding.

A brief introduction to plasma processes is provided by a discussion of their theory, history, and variant forms. Guidelines for matching plasma processes with applications are presented. The choice between plasma and oxy-fuel cutting processes is analyzed in detail; cost-per-foot comparisons are made with high-speed oxy-acetylene and standard natural gas nozzles. Plasma is shown to have a significant economic advantage for high duty-cycle cutting of mild steel up to 1-1/2 inches thick.

A summary is presented of past and probable future developments in high-speed shape cutting machines. Modern machines allow the full economic advantage of plasma cutting to be realized. An efficient material handling system is also required to achieve maximum productivity. Future technology is aimed at increased sophistication of machine control for even greater productivity per man-hour.

The final section describes an investigation of dross formation in plasma cutting of mild steel. The influence of cutting parameters is discussed, and optimum conditions are given for cutting ABS hull steel. Increasing the diameter of the plasma-constricting orifice gives improved cut quality and higher speed on 3/4 to l-inch plate; examples of this technique are shown and disadvantages are discussed.

Cutting performance is found to depend on plate surface condition. In particular, coating with a weldable primer greatly reduces dross formation and expands the operating range for mild steel cutting. Priming of the bottom plate surface is a definite advantage; the top surface is less important, although with a zinc-base primer a very slight speed reduction is recommended.

The effects of cutting parameters and surface condition are summarized in the form of operating guidelines for achieving optimum cut quality.

Table of Contents

Summary

List of Figures iv

List of Tables vi

References vii

1. Introduction 1

2. Plasma Process Fundamentals 2

2.1 Plasma Arc Cutting 2

2.1.1 “Dual Flow” Plasma Cutting 3
2.1.2 “Air” Plasma Cutting 3
2.1.3 “Oxygen Injection” Plasma Cutting 4
2.1.4 "Water Shield” Plasma Cutting 4
2.1.5 “Water Injection” Plasma Cutting 4

2.2 Plasma Arc Welding 5

2.2.1 Needle Arc Welding 5
2.2.2 Keyhole Welding 6

3. Applications 8

3.1 Economics 9

4. Environmental Aspects of Plasma Cutting 11

4.1 Fumes 11
4.2 Noise 12

5. Shape Cutting Machines 14

6. Dross Formation in Mild Steel Cutting 16

6.1 Experimental Procedure 16
6.2 The Dross Curve 16
6.3 Low Speed Dross 17
6.4 High Speed Dross 18
6.5 Top Dross 19

Table of Contents

6.6	Effect of Cutting Conditions	20
6.6.1	Gas Flow	20
6.6.2	Injection Water Flow	20
6.6.3	Standoff	20
6.6.4	Orifice Diameter	21
6.6.5	Gas Type	23
6.7	Effect of Plate Chemistry	23
6.8	Effect of Surface Condition	23
6.9	Conclusions and Operating Guidelines	25

FIGURES

TABLES

List of Figures

Figure No.	Title
1.	Temperature Differences - Constricted Arc
2.	Two Types of Constricted Arc
3.	Positive Cut Angle
4.	Dual Flow Technique
5.	Oxygen Injection Technique
6.	Water Injection Technique
7.	Swirl Injection Nozzle
8.	Direction of Cut
9.	Needle Arc Welding Schematic
10.	Typical Cutting Speeds
11.	Torch Sequences for Beveling
12.	Typical Cutting Costs
13.	Pantograph-Type Cutting Machine
14.	Coordinate-Drive Gas Cutting Machine
15.	Numerically Controlled Cutting Machine
16.	Direct Numerical Control Schematic
17.	Schematic Dross Curve
18.	Dross Curve, l/2-inch Stainless Steel
19.	Cut Contour vs. Speed
20.	Dross Curve with Contour Information
21.	Schematic Cuts at Extreme Speeds
22.	Low Speed Dross
23.	Kerf Width: 3/8-inch Steel
24.	Kerf Width: l/2-inch Steel
25.	Kerf Width: 3/4-inch Steel
26.	High Speed Dross
27.	Dross at High and Low Speed Limits
28.	Dross Weight vs. Speed, Stainless Steel Sheet
29.	High Speed Cutting
30.	Dross Curve vs. Cut Water Flow
31.	Dross Curve vs. Standoff
32.	Kerf Width vs. Standoff
33.	l-inch Steel: 400 Amperes
34.	l-inch Steel: 500 Amperes
35.	l-inch Steel: 550 Amperes
36.	3/4-inch Steel: 375 Amperes
37.	3/4-inch Steel: 500 Amperes
38.	3/4-inch Steel: 580 Amperes
39.	Cross-Section of Figure 38
40.	Dross Curves, 1022 Steel

List of Figures

Figure No.	Title
41.	l-1/2-inch Steel: 600 Amperes, 28 IPM
42.	l-1/2-inch Steel: 600 Amperes, 30 IPM
43.	l-1/2-inch Steel: 720 Amperes
44.	Stainless Steel, Conventional Cut
45.	Effect of Scale Removal
46.	Effect of Iron-Oxide Primer Removal
47.	Effect of Zinc Primer Removal
48.	Effect of Zinc Primer on Sandblasted Plate
49.	Effect of Zinc Primer on Scaly Plate
50.	3/4-inch ABS Steel, 20 IPM
51.	3/4-inch ABS Steel, 50 IPM
52.	3/4-inch ABS Steel, 70 IPM
53.	Dross Curves, 3/4-inch ABS Steel
54.	Dross Curves, l-inch ABS Steel
55.	Dross Curves, 5/8-inch ABS Steel
56.	Dross Curves, l/2-inch ABS Steel
57.	Effect of Surface Finish

List of Tables

I. Water Injection Cutting Conditions

II. Welding Arc Lengths

III. Needle Arc Welding Conditions

IV. Keyhole Welding Conditions

V. Chemical Analyses of Plates Used

References

1. The Welding Environment (American Welding Society, Miami) 1973.

2. "Occupational Safety and Health Standards," Section 1910.93 (The Federal Register, Vol. 39, No. 125) 1974.

3. "Plasma Cutting of Non-Alloy Steel and HT-Steel: Economy, Quality, and Industrial Hygiene" (The Danish Welding Institute, Copenhagen) 1975.

4. J. A. Hogan, "Cutting Characteristics of a 5X12-52WA Water Injection Nozzle" (Union Carbide Internal Progress Report) August 15, 1970.

5. B. Gross, B. Grycz and K. Miklossy, Plasma Technology (American Elsevier Publishing Co., New York) 1969, page 338.

6. P. J. Mayo and J. Lawton, "The Formation and Removal of Dross during Plasma-Torch Cutting of Thin Gauge Stainless Steel" (Electricity Council Research Centre, Liverpool, England) 1971.

7. Welding Handbook (American Welding Society, Miami) 1973, chapter 3.

8. R. H. Willgohs and R. B. G. Yeo, "Weldability of Type 304 Stainless Steel Produced by the Argon-Oxygen Decarburization Process" (Union Carbide Internal Report) 1973.

9. C. Bolt Andersen, "Development of a New Thermal Cutting Technique," Metal Construction and British Welding Journal, June 1974, Vol. 7, pp. 194-200.

10. "Test Operation of PCM-7 Plasma Cutting Machine" (Mitsubishi Heavy Industries, Ltd., Kobe Shipyard) 1973.

11. L. S. Darken and R. W. Gurry, Physical Chemistry of Metals (McGraw-Hill, New York) 1953, page 128.

1. INTRODUCTION

Plasma arc cutting, which was developed 20 years ago for the cutting of stainless steel and aluminum, is now being widely accepted in industry as a high-speed, quality performance tool for processing carbon steel up to 1-1/2 inches thick. Recent improvements in plasma arc cutting equipment and advances in arc constriction techniques render cut surface qualities most suitable for fabricating and welding. High speed shape cutting machines under the guidance of numerical controls or high performance photocell tracers take full advantage of this process' extra fast cutting capabilities so as to make it more than competitive, economically, with the better known oxy-fuel gas process. At the same time, dimensional tolerances can be maintained to permit the close fit-ups necessary for most efficient welding.

Plasma cutting was the major subject of a program sponsored by the Maritime Administration; this report is the conclusion of that program. The program was concerned with applying to the shipbuilding industry the latest technology in high speed shape cutting machines, plasma welding, and plasma cutting. The following objectives have been accomplished as set forth in the original proposal

(a) Establish cutting conditions for alloys and thicknesses representative of ABS ship steel.

(b) Calculate cutting costs based on the cutting conditions, known consumable usage rates, and representative labor costs. Compare plasma cutting cost to those for standard and high-speed oxy-gas cutting nozzles on a cost-per-foot basis.

(c) Visit several shipyards to determine potential plasma cutting and weldin applications. The locations visited were Avondale Shipyard, Litton Shipyard, NASCO, Newport News Shipbuilding, Sun Ship and Todd Shipyard.

(d) Investigate the mechanism of dross formation in plasma cutting of mild steel. Establish general guidelines for reducing dross formation by studying the influence of plate chemistry, surface condition, and process parameters.

This report presents the results of those investigations. In addition sectio are included on the theory of plasma processes and process variations, and on environmental hazards of plasma cutting.

2. PLASMA PROCESS FUNDAMENTALS

In the early 1950's, it was discovered that the properties of the open arc could be greatly altered by directing an electric arc through a nozzle located between an electrode (cathode) and the work (anode). Instead of diverging into an open arc, the arc is constricted by the nozzle into a small cross-section. This action greatly increases the resistive heating so that both the temperature and the voltage are raised. After pas-s-ing through the nozzle, the arc exits in the form of a high velocity, well collimated and intensely hot plasma jet. A comparison of the-plasma arc and the open arc is presented in Figure 1. In this example, both dis-" charges are operating in argon at 200 amps. The plasma arc is moderately constricted by the 3/16-inch diameter nozzle, but operates at twice the voltage and produces a much hotter plasma than the corresponding open arc.

A plasma arc can be used as either a transferred arc or a nontransferred arc as shown in Figure 2. Note that a stream of hot plasma emerges from the plasma arc torch nozzle when either the transferred or nontransferred arc modes are used. In plasma cutting and welding, a transferred arc is generally used since the heat input to the workpiece is most efficient in this mode of operation.

It is possible to further alter the characteristics of the plasma jet by changing the gas type, flow rate, arc current and nozzle size. For example, if low gas flow rates are used, the plasma jet is a highly con-centrated heat source ideal for welding applications. Conversely, if the gas flow rate is increased dramatically, the plasma jet will cut through the workpiece since the velocity of the plasma jet will be high enough to blast away the molten metal created by the plasma arc. In this section, we will consider two of the major plasma arc processes: cutting and welding.

2.1 Plasma Arc Cutting

The plasma jet that is generated by the conventional arc con-striction techniques described above can be used to sever any metal at relatively high cutting speeds. The thickness of the plate can range from 1/8 inch to a maximum thickness depending on both the current capacity of the torch and the physical properties of the metal. A heavy duty mechanized torch with a current capacity of 1000 amps can cut through 7 inch thick stainless steel and 8 inch thick aluminum. However, in most shipyard applications the plate thickness does not exceed 1-1/2 inch. In this thickness range, conventional plasma cuts are usually beveled and have a rounded top edge. In addition, it is necessary to use the proper cutting gas mixture to produce the best results. The cutting gas that is selected will depend on both the type and thickness of metal to be cut.

Beveled cuts are a result of an imbalance in heat input into the cut face. As shown in Figure 3, a positive cut angle will result if the heat input, Q, into the top of the cut exceeds the heat input into the

bottom. One obvious approach to reduce this heat imbalance is to apply the arc constricting principle described in Figure 1: increased arc constriction will cause the temperature profile of the plasma jet to become more uniform and, correspondingly, the cut will become more square. Unfortunately, the conventional approach of constricting the arc with a water cooled copper nozzle is limited by the tendency to establish two arcs in series - electrode to nozzle, and nozzle to work. This phenomenon is known as "double arcing" and can damage both the electrode and nozzle. Double arcing most frequently occurs during arc starting since no conductive path has been established through the constricting passage. The tendency to double arc can be reduced by programming both arc current and the cutting gas during the start. This technique, however, is complicated and has proven difficult to implement in the field.

Several process variations have been developed during the last several years to improve the cut quality in 1/8 inch to 1-1/2 inch thickness range. Recent work has focused on achieving quality cuts on mild steel, since the high cutting speeds associated with plasma make it economically attractive. Each of these process variations is described below. The last process variation, water injection plasma cutting, will be discussed in greatest detail since this innovation has been the most significant breakthrough in cutting of mild steel.

2.1.1 "Dual Flow" Plasma Cutting

The dual flow technique, developed around 1965; is a slight modification of the conventional plasma cutting process. Essentially it incorporates the same features as conventional plasma cutting except that a secondary shield gas is added around the nozzle (Figure 4). Usually the cutting gas is nitrogen and the secondary shielding gas is selected according to the metal to be cut. Secondary shield gases typically used are: mild steel - either air or oxygen; stainless steel - $C0_2$; aluminum - argon-hydrogen mixture. Cutting speeds are slightly better than with conventional cutting on mild steel; however, cut quality is inadequate for many applications. Cut speed and quality on stainless steel and aluminum are essentially the same as with the conventional process. This approach does, however, allow the nozzle to be recessed slightly within a ceramic gas cup; cooling" provided by the shielding gas protects the ceramic from the intense heat radiated by the arc. The recessed nozzle feature protects the nozzle from double arcing to the workpiece.

2.1.2 "Air" Plasma Cutting

Air cutting was introduced in the early 1960's for cutting mild steel. The oxygen in the air provides additional energy from the exothermic reaction with molten steel; this additional energy increases cutting speeds by about 25%. Although the process can also be used to cut stainless steel and aluminum, the cut surface will be heavily oxidized and unacceptable for many applications.

Special electrodes, made of zirconium or hafnium, must be used since tungsten will erode in seconds if the cutting gas contains oxygen. Even with these special electrodes, the service life is much less than what can be achieved with the conventional plasma cutting process.

Although air cutting is no longer used in the United States, it is gaining renewed interest in Eastern Europe, England and Japan. The major supplier of this equipment is Mansfeld of East Germany. Several shipyards in Japan are known to be using Mansfeld air cutting equipment; however, the electrode life averages around 1.7 hours which is low by most standards. A Soviet designed plasma cutting system has also gained some recognition in Western Europe and Japan. Both the performance and design are very similar to the Mansfeld system's.

The major reason for the popularity of air cutting in Eastern Europe appears to be the lack of an efficient gas distribution network, making the cutting gas a major cost component. In the United States, the reduced electrode life more than offsets the "free" cost of air cutting gas.

2.1.3 "Oxygen Injection" Plasma Cutting

This process refinement circumvented the electrode life problem associated with air cutting by using nitrogen as the cutting gas and introducing oxygen downstream in the nozzle bore as shown in Figure 5. This process is used exclusively on mild steel and increases cutting speed by about 25% if the optimum gas mixture is used (80% N_2-20% O_2). The major disadvantages are lack of cut squareness, short nozzle life, and limited versatility (mild steel only). Although this process is still being used at some locations, it has been almost entirely displaced by water injection cutting.

2.1.4 "Water Shield" Plasma Cutting

Water shield plasma cutting is similar to dual flow except that water is substituted for the shield gas. Cut appearance and nozzle life are improved because of the cooling effect provided by the water. Cut squareness, cutting speed and dross tendency are not measurably improved because the water does not provide additional arc constriction.

2.1.5 "Water Injection" Plasma Cutting

Water is introduced inside the constricting passage to provide additional arc constriction as shown in Figure 6. Two modes of water injection have been developed: radial injection - the water impinges the arc with no swirl component; swirl injection - the water is introduced as a vortex swirling in the same direction as the cutting gas. The increased arc constriction provided by the water improves cut squareness and increases cutting speed. The water also protects the nozzle since it provides cooling at the point of arc constriction. Both radial injection and swirl injection methods perform essentially the same when set properly; however, swirl injection, because it has sufficient angular speed to maintain a stable and uniform film, is not as sensitive to variations in cut water velocity.

In swirl injection cutting, water is tangentially injected into a swirl chamber as shown in Figure 7. The function of this swirl chamber is to stabilize and direct the water flow around the arc. Despite the intense temperature generated by the arc, most of the water exits from the nozzle in

the form of a conical spray which cools the top surface of the workpiece, One property of these cuts is that when viewed in the direction of the cut, as shown in Figure 7, the right side of the kerf is square and the left side of the kerf is slightly beveled. This feature is not caused by water injection; rather, it results from the cutting gas which is swirled in a clockwise direction, causing more of the arc energy to be expended on the right side of the kerf. In shape cutting applications, this means that the direction of travel must be selected to produce a square cut on the part being saved.

On the annular shaped part shown in Figure 8, it is necessary to travel in a clockwise direction to make the outside cut so that the saved piece is always on the right side of the kerf. Similarly, the inside cut must be made in a counterclockwise direction to maintain a square edge on the inside of the part. Most applications, like the one shown in Figure 8, discard the beveled side of the cut. Therefore, it is only necessary to consider the right side of the cut in evaluating squareness. Certain applications, such as mirror image cutting, require the high quality side to be on the left. Special "reverse swirl" components are used in this instance. This conversion simply requires changing the nozzle and the gas liner (component that swirls the cutting gas).

Water injection plasma cutting offers some distinct advantages over both conventional plasma cutting and the process variations described above. These advantages are: relatively square cuts at high cutting speeds; smooth, clean cut face; dross free cuts on most materials including mild steel; increased nozzle life since the ceramic bottom piece insulates the nozzle, thereby preventing double arcing; use of one cutting gas, nitrogen, for all metals. The cut angle on the high quality side will usually be within two degrees of square and will seldom require machining or finishing. Typical cutting conditions are presented in Table I.

Cutting conditions will vary with material type and thickness. By far, the most difficult metal to cut square and dross free is mild steel; aluminum and stainless steel are relatively easy to cut. Typical cutting conditions are presented in Table I for the Linde PT-15 water injection (swirl) torch. A more detailed discussion of cutting mild steel will be covered in section 6.

2.2 Plasma Arc Welding

There are two modes of operation possible in plasma welding: the melt-in mode and the keyhole mode. The melt-in mode utilizes relatively low orifice gas flows so that a quiescent weld puddle is produced. This mode of operation offers particular advantage in welding light gauge metal sheet ranging from .001 to .062 inch thick because the low current plasma jet forms a very stable, controllable, needle-like arc. This mode of operation is often referred to as "microplasma"or "needle arc." The keyhole mode of operationon requires moderate currents and relatively high gas flows. In this case, the momentum of the plasma jet is sufficient to penetrate through the weldment to form a deep, fully penetrated weld in one pass. Since these modes of operation are so totally different, each will be handled separately.

2.2.1 Needle Arc Welding

Manual plasma arc welding was developed to obtain a very stable,

controllable arc at low currents for welding thin metal. This process uses a continuously operating pilot arc within the torch to provide a constricted arc which is stable at currents as low as one amp.

Figure 9 shows a diagram of the plasma needle arc welding system. The basic elements of the torch are the electrode and the orifice. A small flow of argon is supplied through the orifice to form the arc plasma. Shielding of the arc and the weld is obtained from a second gas flow through the gas lens and cup assembly. Shielding gas can be argon, helium or mixtures of argon with either hydrogen or helium.

When compared with a gas tungsten-arc, the low current plasma arc or jet has improved directional properties, improved arc stability, and greatly reduced sensitivity to variations in torch-to-work spacing. In addition, contamination of the weld by tungsten is avoided because the tungsten electrode is positioned behind the nozzle. Similarly there is no chance of contaminating the electrode either by accidentally dipping it into the weld puddle or by touching it with the filler metal. Thus arc stability can be maintained.

At very low currents, the plasma needle arc process has special merit for the fusion welding of foils. Manual welding of this thickness represents a significant departure from previous practice with the gas tungsten-arc process, which requires the torch movement to be precisely mechanized. With either process a smooth fusion weld is produced. Table II lists the arc lengths and tolerances for changes in arc length for both the gas tungsten and needle arc processes when operating in the 10 amp foil welding range. Note that the needle arc is ten times longer than the gas tungsten-arc; i.e., 0.25 vs. 0.025 inch. The needle arc tolerance (± 1/16 inch) is more than ten times the gas tungsten-arc tolerance. Thus the needle arc process makes it quite easy to weld foils manually. Typical low current welding conditions are shown on Table III. In all cases, the orifice gas used for low current welding is argon at 1/2 CFH flow through a 0.030-inch diameter nozzle orifice.

The advantage plasma offers on gauge thickness materials has little or no application in shipbuilding. The inner stainless steel liner used in the LNG membrane tank design (Newport News) is the only possible application that has been noted thus far. In this instance, TIG will be employed since the entire fabrication technique is licensed and specifies the TIG process.

2.2.2 Keyhole Welding

In plasma arc welding, the term "keyhole" has been applied to a hole that is produced at the leading edge of the weld puddle where the plasma jet displaces the molten metal, allowing the arc to pass completely through the workpiece. As the weld progresses, surface tension causes the molten metal to flow in behind the keyhole to form the weld bead. Moderately high orifice gas flows are required to establish the keyhole condition: typically 1-20 CFH. Suitable gases are argon, a mixture of argon and hydrogen, or argon and helium, depending on the application. As in the case of the low current needle arc torch, shielding gas is also provided to protect the weld puddle.

Keyholing can be obtained on most metals in the thickness range of 3/32 inch to 1/4 inch and is one of the chief differences between the plasma arc and gas tungsten-arc processes. Presence of the keyhole, which can be

observed during welding, gives a positive indication of complete penetration. Typical welding conditions for square butt joints in mild steel, stainless steel and titanium are shown in Table IV. Note that titanium has an upper thickness limit of 1/2 inch instead of 1/4 inch as in the case of most other metals. The reason for this difference is that titanium has a high surface tension/density ratio. This ratio is a good indicator of upper keyhole thickness limit, since the surface tension supports the weld puddle and the weight of the puddle acts to collapse it.

The major drawback of this process in shipyard applications is its limited thickness range. Also, for the majority of joint designs, submerged arc welding provides higher welding speeds and is less sensitive to variations in fit up and in plate surface condition.

3. APPLICATIONS

The original intent of this phase of the program was to analyze several specific applications in terms of process advantages, limitations, alternatives, and economics. It was decided, after visiting several of the member shipyards, to treat the subject of applications on a more general basis. This approach is less restrictive and does not require information often considered proprietary.

Plasma cutting appears to be well-suited for shape cutting applications where contour beveling is not required. These applications include: bulkheads, webs, stiffeners, deckplates, etc. Multiple torch cutting is especially advantageous in this sort of application if high duty cycles can be maintained.

Plate edge preparation is another potential application for plasma cutting. Although plasma plate edge preparation is limited to single torch beveling commercially, there is no technical reason why double or triple torch beveling cannot be applied if the part is straight or has a large radius of curvature. Contour beveled parts with a small radius of curvature are not practical with today's equipment since the total nozzle separation for a three torch bevel head would be at least six inches.

The most important parameters to determine in analyzing a potential application for plasma cutting are plate thickness and duty cycle. If the plate thickness is such that there is no major speed advantage with plasma, obviously a switch to plasma is not merited. As illustrated in Figure 10, plasma cutting speeds are inversely proportional to plate thicknesses. The equation,

$$s = 40/T \qquad (1)$$

closely approximates the relationship between cutting speed, S in inches per minute and plate thickness, T in inches, for mild and stainless steel. Aluminum follows the same relationship except the cutting speed is roughly 25% faster than steel. It should be noted from Figure 10 that plasma cutting holds a significant speed advantage over the oxy-acetylene process up through 1-1/2 inches thickness.

In beveling applications the cutting speed is determined by the width of the cut face rather than the plate thickness. For example, a 45° bevel cut on l/2-inch plate must be set for 3/4-inch plate since the width of the cut face is .71 inch. The cutting speed of the beveling operation on mild steel can be estimated by applying a modified version of equation (1).

$$S = 40 \cos\alpha / T \qquad (2)$$

The term α is the bevel angle measured with respect to the vertical.

If double or triple torch beveling is required, the cutting conditions must be adjusted to suit the travel speed of the slowest torch. The torch sequences for various beveling configurations are illustrated in Figure 11. These sequen are the same as those for oxy-acetylene beveling; with both processes the quali cut is made without-requiring the jet to cross a previous kerf. For plasma cutting, these sequences also have the advantage of minimizing standoff of each torch.

3.1 Economics

The most costly element in a cutting operation is labor. Other factor such as power, gas, and nozzle and electrode consumption, account for 15% to 25 of the total cutting costs. Any slight increase in productivity (speed, duty cycle, additional torches, etc.) will greatly reduce the cost per foot of cut.

It is interesting to note that a rough estimate of the cutting costs c be obtained simply by dividing the average length of plate cut per hour into the cost of labor and overhead. For example, according to Figure 10, l/2-inch steel can be cut at 90 ipm. Assuming that the-cost for labor and overhead is $15 per hour and the duty cycle is 50% (arc is on four out of eight hours), the approximate cost is calculated as follows:

$$\text{Length per hour} = \frac{(90 \text{ in./min.})\ (60\text{min./hr.})\ (0.5 \text{ arc hrs./hr.})}{(12 \text{ in./ft.})}$$

$$= 225 \text{ ft./hr.}$$

$$\text{Cutting cost} = \frac{\$15/\text{hr.}}{225 \text{ ft./hr.}}$$

$$= .067 \text{ \$/ft. or } 6.7 \text{ ¢/ft.}$$

For cutting thin material (when power and consumable costs are low), the actual cost will be about 15% higher than this estimate. For heavier plate the increa can be as much as 25% since the power consumed is considerably greater.

A more exact estimate of cutting cost can be obtained by applying equation (3).

$$W = \frac{20}{S}\left(100\,\frac{L}{ND} + G + H + J + K\right),$$

where:

W = Cutting cost (¢/ft.)
N = Number of torches
S = Cutting speed (in./min.)
L = Labor and overhead ($/hr.)
D = Duty cycle (%)
G = Gas cost per torch ($/arc hr.)
H = Nozzle cost per torch ($/arc hr.)
J = Electrode cost per torch ($/arc hr.)
K = Power cost per torch ($/arc hr.).

Except for the power cost K, the parameters listed above are straightforward to calculate. When calculating the cost of power, two contributions must be considered: the energy charge and the demand charge. The energy charge is based

on the total consumption of energy (kilowatt-hours). The demand charge is a monthly premium paid for the increased peak load (kilowatts) due to the plasma installation. Both are included in equation (4); the demand charge is divided by the number of arc hours per month to get cost per arc hour.

$$K = \left(\frac{VI \times 10^{-3}}{E}\right)\left(Q + 23\,\frac{R}{DMX}\right), \qquad (4)$$

where:

V = Arc Voltage (volts)
I = Arc current (amperes)
E = Efficiency of cutting power supplies (typically 0.9)
Q = Energy charge ($/kw-hr.)
R = Demand charge ($/kw)
D = Duty cycle (%)
M = Number of working hours per day
X = Number of working days per week.

The power factor of the cutting power supplies is not included in this equation, since its effect depends on the methods of the local power company. For example, the power company might charge a one-time fee when the supplies are installed if the plant's overall power factor is reduced.

A "typical" cutting cost is impossible to estimate since the parameters discussed above depend greatly on location. It is possible, however, to make a relative cost comparison with oxy-fuel cutting for a hypothetical user, as is shown in Figure 12. A rate of $15 per hour for labor and overhead and a 50% duty cycle were assumed. Costs for gas, power, and torch consumables were calculated using the most recent rates for large industrial accounts. In the case of mild steel cutting, the cost advantage of plasma is 4 to 1 on 1/4-inch plate and 2 to 1 on 1-1/2-inch plate.

4. ENVIRONMENTAL ASPECTS OF PLASMA CUTTING

4.1 Fumes

The safe concentration of airborne pollutant, averaged over an eight-hour day, is the threshold limit value (TLV). For particularly hazardous contaminants, a maximum concentration is also specified that cannot be exceeded at any time. Regulations in the United States[1,2] are the following:

Particulate Fumes	TLV (mg/m^3)
Iron oxide	10
Aluminum oxide	10
Chromium oxide	0.1
Zinc oxide	5
Manganese	5

Gases	TLV (ppm)
Nitrogen dioxide	5
Carbon monoxide	50
Ozone	0.1

Regulations in some European countries are more severe[3]. For example, iron oxide's TLV is 5 mg/m^3; chromium oxide 0.05; ozone 0.05 ppm; and nitrogen dioxide is specified at 5 ppm maximum rather than average concentration.

For mixtures of contaminants, the total effect on personnel is assumed to be additive. The total exposure Em is calculated according to:

$$E_m = \frac{C_1}{TLV_1} + \frac{C_2}{TLV_2} + \cdots + \frac{C_n}{TLV_n}.$$

This weighted sum cannot exceed unity.

A single plasma torch has the potential to exceed all the TLV's listed above, according to worst-case measurements taken from the cutting table exhaust. In a typical industrial installation, however, the levels approximately equal the TLV's even without pollution control measures. For example, the NO_2 level in the worst case can be as high as 90 ppm. When cutting is done in a high bay area, this value drops to 5 ppm at the operator's position 10 feet from the torch.

In the early years of plasma cutting, a downdraft exhaust ventilation system was the preferred means of pollution control. The recommended exhaust flow was 150 CFM per square foot of cutting table area. To reduce the size of the total exhaust system, two methods were used: (1) covering the unused area of the table; (2) building the table in compartments with movable baffles. Venti

lation systems are particularly effective in removing gaseous contaminants, and reduce particulate fumes to levels below their TLV's.

The accepted pollution control device now is the water table, patented by Hypertherm. The cutting table is filled with water up to the bottom surface of the plates. The high-speed gases emerging from the plasma jet produce turbulence in the water. 99.5% of the fumes particles are trapped, in a manner similar to the operation of a scrubber in an air pollution control system. The water table is less efficient in removing gases, but gas levels are still below their TLV's.

The following example[3] illustrates the relative effectiveness of ventilation and water table methods. Measurements were made 9 feet from the torch, while water-injection cutting 11 mm thick zinc-primed steel at 275 amps and 70 ipm. These-values are higher than would be obtained in a typical industrial site for two reasons: (1) tests were done in a laboratory room of relatively small volume without added room ventilation; (2) the values correspond to 100% duty cycle.

	Without Control	With Ventilation	With Water Table
NO_x, ppm	3.8	0.7	3.2
CO, ppm	< 5	< 5	< 5
03, ppm	<0.005	<0.005	<0.005
$Fe_2$03, mg/m3	15.07	6.77	3.61
ZnO, mg/m^3	1.18	0.97	0.13
Mn, mg/m^3	0.29	0.20	0.04
Approximate total exposure Em	2.7	1.16	1.14

Pollution levels increase with increasing current. The use of air as the cutting gas increases the amounts of metal oxides and NO_x. Water-injection torches lie about midway between lower-current types and air-cutting torches.

4.2 Noise

The amount of noise generated by a plasma cutting torch depends mostly on the current. One PT-7 torch operating at 425 amps in the water injection mode generates 108 dBA when measured at a distance of six feet. At 750 amps the noise level can be as high as 115 dBA, while at 300 amps the noise level would be 102 dBA (measured six feet from the torch). The noise lies within a frequency range of 5000 to 20,000 Hertz; ultrasonic noise is not at all a hazard.

It is important to realize that noise will only be a problem in the immediate cutting area since the noise level will rapidly diminish as you move further away from the torch. The following equation describes the rate of' noise attenuation as a function of distance:

$$I = I_0/D^2$$

I = calculated intensity
I_0 = source or measured intensity
D = distance away from source

In other words, the sound intensity is reduced by one quarter as the distance away from the source is doubled. The next equation describes this change in terms of decibels:

$$dB=10 \log (I/I_0)$$

Since the intensity, I, is reduced by 1/4 when the distance away from the source is doubled, the preceding equation reduces to:

$$dB = 10 \log (41_0/I_0) = 10 \log 4 = 6$$

Therefore, each time the distance from the source or where the in measurement was made is doubled, the decibel reading will be reduced by six. The measurement of 105 dBA (the "A" in dBA refers to the scale used on the instrument used to make the measurement) at 6 ft. would only be a 99 dBA at 12 ft., 93 dBA at 24 ft., and 87 dBA at 48 ft. Consequently, the actual exposure limit will depend on both the intensity of the source and the distance from the source. Similarly, doubling the number of torches increases the noise level by 3 dB.

The maximum acceptable noise level, according to OSHA regulations, is 90 dBA for 8 hours continuous exposure; for 4 hours, 95 dBA; for 2 hours, 100 dBA. Thus plasma cutting does produce unacceptable noise levels; an operator 6 feet from the torch would experience approximately 108 dBA; the allowed limit is 95 assuming a 50% duty cycle.

A method for reducing noise to acceptable levels is the water muffler. This is a nozzle attached to the torch body that produces a curtain of water around the torch front end. The muffler is always used in conjunction with a water table; water from the table is pumped through the nozzle at a rate of 18 GPM. The combination of the water curtain at the top of the plate and the water contacting the bottom of the plate effectively encloses the arc in a sound-deadening shield. The noise output is reduced by roughly 20 dBA.

This technique should not be confused with water injection or water shielding (described in section 2.1); neither uses a sufficient flow of water for noise reduction.

5. SHAPE CUTTING MACHINES

Developments in plasma cutting have been paralleled by improvements in cutting machines. The evolution of the process into a high-speed production tool generated a demand for high-capability cutting machines. Without such machines the full economic advantages of plasma could not be realized, and there could be no significant swing from oxy-fuel processes.

The enormous advances in cutting machines can be easily seen by comparing the present and future state-of-the-art with the machines of 20 years ago. In the early 1950's when the original patents for the plasma process were being issued, the typical cutting machines were pantograph types. Some used a primitive silhouette optical tracing system, but most had magnetic or manual steering devices (see Figure 13). The drive was generally provided directly from the template surface or edge, resulting in barely adequate speeds for oxy-fuel cutting and so little force behind the motion that stalling was considered a normal hazard. The selling price of these simple tracers was six to twenty times less than that of today’s sophisticated machines.

Features that are now considered basic requirements for good machine performance did not appear until the end of the 1950's: coordinate drive (individual drive unit for each rectilinear axis), high motion torque for quick response, rigid machine construction for the high harmonic frequencies required at high gains, and many others. At that time machines with these features, such as the one shown in Figure 14, were considered almost revolutionary and perhaps too rich for the existing market. Plasma cutting was then no more than a novel tool for severing non-ferrous metals, and was not a significant factor in that market.

The early sixties saw the coupling of numerical control to oxy-fuel cutting machines. This was the one big step that lifted shape cutting machines from a primitive tool to a precision machine. From that time until today, a process of continual change has led to the present highly sophisticated automatic production tool. Figure 15 is an example of a recent machine.

Present control systems rely heavily on computer technology; almost all of the machine direction is generated via a computer program rather than by hardware. These computer numerical controls (CNC) have the advantages over older controls of greater reliability, expanded capability, lower cost, and last but not least the ease of connecting several units to a central processor as a direct numerical control (DNC) system. This approach is illustrated in Figure 16. Here the "host computer" is the source of part programs as an output of computer lofting. The data flow through the system control computer to a mass storage device such as the "flexible disk." The DNC operator can command the programs to be plotted for visual verification and then to be printed or displayed on the CRT. He can make minor program corrections through the keyboard, and code the program for access by machine operators. The DNC approach completely eliminates the need to produce perforated tapes.

The productivity potential of a numerically controlled, multi-plasma shape cutting machine is staggering. In fact, the most common problem associated with new installations of this type is material handling; the methods normally accepted for oxy-fuel machines cannot be retained. Not only is there a manyfold increase in output, but the material flow is concentrated through the very small area of the machine cutting tables. The most common practice to alleviate this problem is to provide sufficient table length to allow cutting in one area while loading and unloading work in one or more other areas. Other remedies involve improvements in the cutting table design. These include: retractable stops for quick plate alignment; fixed plate supports to prevent their dislocation during unloading; a relatively fine mesh under the supports to minimize scrap accumulation; and the capability of rapid water level adjustment in water tables to facilitate the operator's work. Obviously consideration must also be given to the requirements for cranes and other material handling devices.

The cutting machine technology of the future is expected to move toward the ultimate in any automatic machine - adaptive control. Plasma cutting in particular lends itself to almost complete automation. There is no "flame" adjustment, and the machine can easily monitor the existence of a transferred arc and thereby sense when cutting occurs. The large difference in voltage between arc-off (open circuit) and arc-on is used to control machine motion.

A more accurate monitoring of the arc-voltage provides a means of regulating torch height. This recent development illustrates the trend toward adaptive control. Previous methods of height control used external proximity devices, such as capacitance, pneumatic, or magnetic sensors. The inadequacy of those devices, particularly in the presence of water mufflers, prompted the development of a control dependent upon the actual arc voltage. Since the voltage varies not only with torch standoff but also with speed, plate thickness, and current, the present design samples the voltage a couple of seconds after ignition to insure stabilization of these other parameters.

In conclusion, it can be seen that today's success in plasma cutting is due as much to the improvements in shape cutting machines with high accurate contouring speeds and automatic control of the process as it is due to the improvements in the plasma equipment.

6. DROSS FORMATION IN MILD STEEL CUTTING

Plasma cutting has reached a level of quality and reliability to become an accepted production tool for fabrication of mild steel plate. The greatest remaining problem is an annoying by-product called dross – a tenacious deposit of resolidified metal at the bottom edge of the cut. Although removal of the dross is usually a simple task, the extra processing step means added labor cost and reduced material handling efficiency.

This section presents the results of a study of the important variables in dross formation. The discussion of the effects of process and material variables will be preceded by background and theory, and concluded with a summary of operating guidelines.

6.1 Experimental Procedure

All experiments were performed with a Union" Carbide PCC-8 plasma cutting control mounted on an OM-48 side beam carriage which allowed only straight-line cutting. Most of the work used a PT-15 torch, which is designed exclusively for water-injection cutting with nitrogen gas. A few tests used the PT-7 torch, for example to compare cutting with air as the plasma gas. Both torches incorporate a clockwise gas swirl as discussed in section 2.1.

The ABS plate used in the investigation was supplied by Bethlehem Steel Corporation, Sparrows Point, Maryland. The plates were ABS quality hull structural steel with three types of surface preparation: unprepared (mill scale), sandblasted, sandblasted and primed (zinc dust primer). Chemical analyses of all plates are given in Table V.

6.2 The Dross Curve

Discussion of the mechanisms of dross formation will be aided by first defining a "dross curve." This method of data presentation was first used by J. A. Hogan as a tool for evaluating nozzle designs. A series of cuts are made at varied travel speeds; all other parameters are held constant. A minimum speed, the low-speed limit, is found such that any lower speed results in dross formation. Similarly a high-speed limit is determined, which is the maximum speed for a dross-free cut. The range of speeds between these limits is called the dross-free interval.

For graphic presentation, the limits thus obtained are plotted versus arc current by repeating the series of measurements described above. Other process parameters could of course be used as the second variable (examples will be given in section 6.6), but the others are normally held constant throughout the thickness range of a given nozzle. A schematic dross curve is shown in Figure 17. The region contained within the boundaries is the optimum operating space for the chosen set of fixed parameters. The upper limit,

determined by the current rating of the nozzle, is usually not included. Also shown is a "loss of cut" line at the right; this is the limiting speed for complete penetration, beyond which the plasma jet "kicks back." Two important characteristics of the curve should be noted: (1) the low-speed limit shows little variation with current; (2) the high-speed limit and loss-of-cut line are close and approximately parallel.

Figure 18 is a dross curve for l/2-inch thick 304 stainless steel, taken from reference 4 where it was used to evaluate a prototype water-injection nozzle. The dross-free interval is very wide, 96 inches per minute (ipm) at 250 amps for example. Unfortunately a perfectly square cut edge cannot be obtained throughout this wide range. High speed gives a rounded top and a beveled edge to the cut. Low speed gives a concave surface and a slight negative bevel. It has been shown that there is a simple monotonic dependence of cut squareness on the position of the operating point within the dross curve. The numerous cuts which went into Figure 18 were graded by assigning a number from -3 to +3 to the face contour; a perfectly square cut was rated zero. Typical cut contours are sketched in Figure 21, and at the left of Figure 19 along with their "contour grades."

The abscissa in Figure 19 is "interval speed": travel speed normalized to the dross-free interval. The origin is the low-speed limit; 100% is the high-speed limit. The resulting plot is linear within experimental error. Note that there is no explicit reference to arc current. Interval speed is the "norma coordinate," and current acts only to expand the operating range. Figure 19 shows that a square cut (zero contour grade) occurs at 44% interval speed for the 1/2 inch stainless. A useful rule of thumb for all cases is that the optimum cut is obtained at about 50% interval speed.

A complete description of the material's cutting performance is shown in Figure 20, with the contour information added to the original dross curve. Proposed mechanisms for dross formation must take into account the close correlat of cut contour with the dross curve.

6.3 Low Speed Dross

Low cutting speed on carbon steel produces a heavy "bubbly" deposit at the bottom of the kerf; Figure 22 is an example. In extreme cases the bottom edges of the kerf are welded together such that separation of the pieces is impaired. Such severe dross is-normally seen only-when the plate thickness approaches or exceeds the capacity of the nozzle. In such cases the problem is sometimes identified as insufficient penetration. However, close observation during cutting reveals that the plasma jet does penetrate well beyond the bottom of the plate. Close behind the arc can be seen molten metal rejoining and then solidifying. This phenomenon has been described by one writer[5] as follows:

"Insufficient cutting speed causes excessive heat supply to the region of the lower edge; the material is fused over a greater width than that of the directed plasma jet, and therefore it is not completely blown out from the cut. As the torch passes on, the molten metal joins again and forms bridges."

The mechanism suggested by this description is the melting of a greater volume of metal than can be fully removed by the force of the jet. Several factors contribute to an increase in melted volume as speed decreases:

(1) Kerf width increases.

(2) Cut angle (deviation from a square edge) decreases, eventually reaching a slight negative bevel.

(3) The contour of the cut face changes from convex (rounded top) to concave.

On very thick plate, for example five-inch stainless, the kerf width can be four times the orifice diameter. One can observe liquid metal in motion well outside the luminous core of the jet. At such a large radius the jet velocity is very low.

Accompanying the increased volume is a greater proportion of melting at the lower edge of the cut. Figures 23 through 25 give kerf width measurements on three thicknesses of 1022 carbon steel. (Corresponding dross curves are in Figure 40.) The width of the bottom of the kerf shows a greater rate of change than does the top width. The appearance of the cut changes with decreasing speed as sketched in Figure 21. The cut angle decreases, particularly on the left (beveled) side. The angle on the right side changes relatively little at sub-optimum speeds; a negative bevel of more than 2° is rare.

The suggested mechanism for low-speed dross is therefore the expansion of the kerf into those regions where the arc force is minimum: at a large radial distance from the axis of the arc, and at the bottom of the cut. The spatial distribution of the arc force is more important than its maximum magnitude. This agrees with the slight dependence of the low speed limit on current. Note that the bottom kerf width in Figures 23 and 24 also shows relatively little change with current. Another supporting observation is that dross tends to appear first on the left side of the cut as the speed approaches the low-speed limit; Figure 41 is an example. More of the arc energy is expended on the right wall of the kerf because of the clockwise gas swirl.

6.4 High Speed Dross

High speed dross on carbon steel is typically a thin, linear bead of solid metal, as shown in Figure 26. The deposit appears to be a continuation of the fused kerf wall; it is "welded" to the bottom of the cut and is difficult to remove. This is to be contrasted with low-speed dross, which has an appearance much different from the cut face, is separated by a visible parting line, and is easily removed (see Figure 22). At or near the high-speed limit, the deposit can have the form of a light flat spatter as at the bottom of Figure 27. Although the continuity with the cut face is still present, this type can be easily removed by prying up the ends of the pieces; this characteristic has led to the term "fingernail dross."

High-speed dross is rarely encountered in industrial installations. It exists in a narrow speed interval between the high-speed limit and the loss-of-cut line. An operating point in this range is seldom chosen because of the ease of losing the cut in the event of a fluctuation in cutting conditions, and because of the positive cut angle at high speeds.

One of the few references to high-speed dross in previous work appeared in a study of thin stainless cutting[6]. Figure 28, from that report, shows weight of dross as a function of travel speed. The dross-free interval can be seen to

lie approximately between 15 and 20 cm/sec. The quantity of high-speed dross is small, and decreases as the loss-of-cut speed is approached. The curve for "top dross" will be discussed in section 6.5.

The following changes occur as the cutting speed increases from its optimum value:

(1) The heat supply to the lower half of the cut decreases, giving a more positive cut angle. The variation is more pronounced than at low speed; an angle of 40° can be produced in extreme cases.

(2) The efficiency of metal removal increases: a greater volume per second is removed with approximately the same power input.

(3) The lag angle (angle between the exiting jet and the vertical) increases. Near the maximum speed, the tail of the jet begins to "pump": the lag angle oscillates, for example between 60° and 80°, with a period on the order of one second. At a slightly higher speed the cut is lost as the lag agnel approaches 90°.

A possible mechanism for dross formation at high speeds is sketched in Figure 29. The locus of arc attachment points can be seen as "lag lines" on the face of a cut (as in Figure 26). In the lower third of the cut the arc sweeps back steeply. It is probable that the hot gas, with no tendency to attach to the metal walls, leads the arc slightly at the bottom. Thus the small amount of metal melted by the trailing arc is not expelled. This process is suggested by the observations that the lag lines continue smoothly from the face into the dross deposit, and that the dross is not porous as in the low-speed case. The pumping phenomenon would then occur when the end of the already-elongated arc attaches to the dross, giving an effect similar to a temporary increase in plate thickness.

An increase in current provides greater heat supply to the bottom of the cut and decreases the arc lag. Both the high-speed limit-and loss-of-cut speed are increased. An example of the dependence of maximum speed on current is shown in Figure 26; a current reduction of 30 amps moved the operating point across the loss-of-cut line.

6.5 Top Dross

A third kind of defect in plasma cuts is the production of spatter on the top of the plate adjacent to the kerf. An excellent model for' this phenomenon is given in Reference 6. In a cut with a large positive bevel, a considerable gradient in gas pressure exists from the top to the bottom of the cut face due to the changing radial distance from the arc center. The pressure difference is sufficient to cause some molten metal to flow to the top of the face.

Top dross is not a problem with water-injection plasma cutting. A few fine threads can be produced at high speeds or large torch-to-work distance, both of which increase the cut angle. It normally appears along with a rounded top of the cut edge, which is more common in conventional cutting processes.

6.6 Effect of Cutting Conditions

6.6.1 Gas Flow

The previous discussion often referred to lack of arc energy in dross formation. It has been found that the gas flow is not critical to cut quality; it has much less effect than the electrical energy of the arc as determined by current. Variations in gas flow were tried on all plate thicknesses; differences of 20 ft.3/hour (CFH) had no noticeable effect on the cutting performance. This represents a change of 14% from the normal value of 140 CFH for the PT-15 torch with .156 nozzle. Larger deviations are impractical because of the adverse effect on consumable life.

This tolerance to errors in gas flow allows the use of a pressure gauge in plasma cutting equipment as a flow indicator. In the PCC-8, for example, the pressure gauge is accurate to 2 psi, which can cause a flow error of 10 CFH.

6.6.2 Injection Water Flow

The greatly improved cut quality afforded by the water injection technique leads one to expect a strong dependence of dross formation on "cut water" flow. Figure 30 is a dross curve using cut water flow as the second variable. The most important feature is the existence of a minimum flow for dross-free cutting; the minimum here is approximately 0.28 gallons per minute (GPM). A near-maximum dross-free interval is obtained at about 0.33 GPM, and this is the setting recommended for the .156 nozzle. A higher flow serves only to increase the rate of electrode erosion. The optimum cut water flow determined in this way depends primarily on the orifice diameter. For this reason a flowmeter, as opposed to a fixed valve, is used in Union Carbide's latest mechanized cutting control.

The cause of the slight drop in cutting speed at high flow is not clear. Turbulence may begin as the velocity of the confined vortex increases, leading to reduced arc constriction.

6.6.3 Standoff

The standoff distance, measured from the end of the nozzle to the plate surface, is known to affect the cut angle. A large standoff produces a positive bevel; a small one causes undercutting of the face and a negative angle. The resulting contours are very similar to those shown in Figure 21.

The dross curve given in Figure 31 shows a limited range of standoff for an adequate dross-free interval, approximately 1/4 to 7/16 inch. In practice a closer tolerance is desirable to insure a uniformly square edge. The cut angle varies approximately 10° between the limits of 1/8 and 1/2 inch given by the dross curve.

This large variation is apparent in the effect on kerf width (Figure 32). Most of the change occurs at the top of the kerf, unlike the variation with speed. This behavior has a useful side effect: standoff can be used to fine-tune the cut angle in troublesome cases. For example, cutting of very thin plate (under 1/4 inch) with a water-injection torch gives a positive cut angle, because a nozzle with a small enough orifice diameter is not provided

for this infrequent application. The squareness can be improved by using a smaller-than-normal standoff. Conversely, conventional cutting of five to seven-inch thick material tends to undercut the top edge; the solution is to increase the standoff.

The dross formed at a small standoff distance has a low-speed appearance, since a negative cut angle is favored even at relatively high speeds. The reverse is true at a large standoff. Thus the areas on the dross curve representing the two types are skewed, as shown schematically in Figure 32. The exact transition point between the two is difficult to distinguish in experiments.

6.6.4 Orifice Diameter

The industrial user of plasma cutting gives little consideration to orifice diameter when selecting operating conditions. A very limited range of nozzles is made available by the equipment manufacturer, who recommends a single size for a given plate thickness. Nevertheless, the choice of orifice diameter can be important, particularly when the plate thickness is close to the transition between recommended nozzles. The following discussion will emphasize the choice between the .156 and .200 nozzles when using the PT-15. This case arises most frequently (for plate thicknesses near one inch) and shows the greatest effect on quality and economics.

The .156 nozzle is recommended for cutting plate up to one inch thick, using currents up to 400 amps (see Table I). It is possible to obtain square cuts on thicker material, but at the expense of slow travel speed and heavy dross on carbon steel. Improved performance can be obtained by raising the current, but nozzle life will suffer. (The reduction in nozzle life due to excessive current is even more noticeable with other torches, which are more likely to double-arc during starting.) Another disadvantage is the need for an additional power supply, since the largest available supply at present is rated at 400 amps for continuous operation.

Of much more interest is the opposite case: using a larger orifice than necessary. Table I recommends either the .156 or the .200 nozzle on one inch plate. The factors governing this choice are the following:

(1) Cutting speed is much higher with the larger orifice: 60 inches per minute compared to 30.

(2) The .200 nozzle operates at a higher current. This is a disadvantage because of the need for a second 400-ampere power supply. If the user has the extra power supply anyway (for cutting plates thicker than one inch) the increased cost of electricity is more than offset by the greater speed.

(3) Kerf width (at the top) is approximately 20% greater with the larger orifice.

(4) Nitrogen consumption is 29% greater.

(5) The dross-free interval is much wider at the higher current.

To illustrate the last point, Figure 33 through 35 show "tuning fork" samples cut from one-inch 1018 steel. On all such samples, the photograph shows the bottom surface; the top edge was cut from right to left and the bottom edge from left to right, so that each is the square (right) side of the cut. A partial cut was made in the middle, from right to left, to show both sides. The cutting speed in each case was adjusted for optimum squareness.

Figure 33 shows the heavy low-speed type of dross obtained with

the .156 nozzle. The .200 nozzle at 500 amperes gave Figure 34; the dross is smaller in quantity and its appearance is not clearly low or high speed. This is often the case when the operating point is just below the lower boundary of the dross curve. A further current increase to 550 amperes gave the essentially dross-free cut shown in Figure 35. The isolated pieces of dross at the beginning of each cut were caused by excessive arc lag before the arc achieved full penetration. They can be prevented by delaying the start of travel for approximately one-half second after arc ignition; no travel delay was used here. The dross at the start of the middle cut shows definite high-speed characteristics, as is expected with high lag: a smooth transition between the cut face and the dross, with continuous lag lines.

The width at the bottom of the kerf, as shown in the photos, stayed roughly constant. The top width increased 20%, from 0.236 inches at 400 amps to 0:283 at 550 amps. This agrees with the earlier discussion of dross formation mechanisms; low-speed dross is favored when the kerf walls become more nearly parallel. The difference is in the distribution of arc energy, not in its magnitude. Note that the nominal current density (current divided by orifice area) was smaller for the dross-free cut: 1.75 x 104 amps/in.^{2} for Figure 35, versus 2.09 x 104 for Figure 33.

The influence of orifice diameter on the dross curve can be seen in Figure 54. For one-inch ABS plate without primer-coated surfaces, no dross-free interval is shown with the .156 nozzle; the optimum speed is approximately 32 ipm. Using the .200 nozzle, dross-free cuts are achieved at twice the speed. For further illustration, data are also shown for an experimental .173 inch diameter orifice; this size is not commercially available.

The same factors listed above also apply when cutting 3/4-inch plate, with one added point: the .200 nozzle causes a slight rounding of the top edge. This is a common defect when the orifice diameter is larger than required for the plate thickness. The same problem arises when cutting very thin plate with the .156 nozzle, as mentioned in 6.6.3.

Figure 36 shows a tuning-fork sample made from 3/4-inch 1018 steel at 375 amps. The dross is not heavy and is easy to remove; this is a good example of "fingernail" dross. Figures 37 and 38 show the dross-free cuts obtainable with the .200 nozzle. 500 amperes is sufficient for this plate thickness; the higher current gives a wider dross-free interval and higher speed. The top-edge rounding can be seen in Figure 39. The effect of the larger nozzle on the dross curve for 3/4-inch plate can be seen in Figures 40 and 53.

An improvement in speed and quantity of dross with increasing orifice diameter can also be seen on thicker plate. Figures 41 and 42 illustrate the difficulty of obtaining dross-free cuts on 1-1/2-inch steel. The optimum speed has a tolerance of less than 2 ipm; even at the best speed, 30. ipm, a fluctuation in some other parameter may bring on dross (as happened in Figure 42). Such fluctuations may arise from crossing a kerf or plate defect, or from variations in standoff, current, or cut water flow. Figure 43 shows the same plate cut with a larger nozzle. Although the improvement is not as dramatic as on thinner plate, the use of the larger orifice is attractive because the current remains within the 800-ampere capacity of two power supplies.

The difficulty of achieving a dross-free cut on thicknesses greater than 1-1/2 inches further justifies the use of oxy-fuel processes in that range, as recommended in section 3 on economics.

6.6.5 Gas Type

Virtually all plasma cutting of mild steel is done with one of three gas types: (1) nitrogen, with $C0_2$ or water shielding or water injection; (2) nitrogen-oxygen or air; (3) argon-hydrogen mixtures. The first two have become standard for high-speed mechanized applications. Argon-hydrogen (20 to 35% hydrogen) is occasionally used for manual cutting, but dross formation is a problem. A possible explanation for the heavier, more tenacious dross formed in argon is greater surface tension of the molten metal. The surface tension of liquid steel is 30% higher in an argon atmosphere than in nitrogen[7].

Air-cutting gives dross similar to that with nitrogen. Studies of surface tension during welding[8] have shown that a minute quantity of oxygen (a fraction of one percent) is sufficient to reduce the surface tension significantly. That much oxygen is present even in a nitrogen arc. The added oxygen in an air arc apparently has relatively little further effect.

6.7 Effect of Plate Chemistry

The original intention of this study was to correlate dross formation tendency with-chemical composition of the steel. This approach was suggested by the vast difference in cutting performance between carbon and stainless steels That difference can be seen by comparing Figure 18 with any of the dross curves for carbon steel. Even when dross is formed on stainless steel, it is rarely the heavy, bubbly type shown earlier; it typically appears as thin isolated strings. Figure 44 shows the worst dross normally encountered on stainless steel obtained by cutting with a low-current torch with argon-hydrogen gas.

As an aid in correlating composition and dross formation, the material property which looked most promising was liquid surface tension. Liquid iron has the highest surface tension of any of the common metallic elements. This fact might account for the greater difficulty of metal expulsion by the plasma jet and the typically heavy deposits formed on steel.

It was not possible to pursue that direction of research because of the limited availability of mild steel alloys. Only a few alloy types were obtainable, especially in plate form. The study then centered on the effect of surface condition, as will be discussed in the next section.

Compositions of the materials used are given in Table V. No significant differences in cutting performance were seen among the compositions tested.

6.8 Effect of Surface Condition

Shipyard fabricators are familiar with the effect of plate surface condition on oxy-fuel cutting processes. When cutting plates pre-coated with zinc primer, the travel speed must be decreased to avoid loss of cut; the primer apparently interferes with efficient preheating. An iron-oxide primer has been found to reduce slag adherence as compared to sandblasted plate, with no loss of speed.[9]

A few previous studies have pointed out similar effects on plasma cuttir A 1973 Japanese report[10] stated that a primer coating of any kind eliminated dros adherence, and that only the bottom plate surface had an effect. A Danish study

found that primed surfaces inhibited dross, but that a slower speed or higher current was necessary with a zinc-base primer.

For the present work, three types of primers were investigated. Most of the tests involved a zinc-dust primer: zinc dust (79.6%) plus zinc oxide (20.4%) pigment, in an alkyd binder (62.2% pigment by weight). An iron-oxide-in-epoxy primer (popular in Europe) and a yellow zinc chromate were also tried. Plates had been sandblasted prior to coating.

On plates less than 3/4 inch. thick, all primers gave a wider dross-free interval. Although dross-free cuts are easily obtained on those thicknesses of unprepared (scaly) plate, a significant difference could be seen at sub-optimum speeds. Figure 46 shows cuts made in 5/8-inch ship" steel (Danish grade 42); the PT-15 with .156 nozzle was used at 375 amps and 62 ipm. This low speed produced dross where the bottom of the plate had been cleaned. The iron-oxide primer on the other half eliminated dross. The increased dross-free interval due to a zinc primer can be seen in the dross curves for 5/8 and 1/2-inch ABS steel (Figures 55 and 56). Figure 55 also swows the conditions for using the .200 nozzle, but cut squareness is poor as dicussed in section 6.6.4.

On 3/4 to 1 inch thick steel, for which dross-free cutting is difficult, the presence of primer is a definite advantage. Dross is not completely eliminated, but the amount of dross is very small over a wide range of speed. Figures 50 through 52 show 3/4-inch zinc-primed ABS plate cut at speeds of 20, 50, and 70 ipm. At the optimum speed of 50 ipm, a tenacious non-porous dross approximately 1/32 inch long is formed. At 20 ipm the deposit is more objectionable, but a cut in unprimed plate at this very low speed would be welded at the bottom. A slight increase in dross quantity is also seen at 70 ipm. Dross curves are given in Figures 53 and 54.

The effects of the zinc primer on 3/4-inch plate are dramatized in Figures 47 through 49. The first shows the primer partially removed. The second shows primer added to sandblasted plate; the unseen top surface was not primed. Even without previous scale removal, the zinc primer reduces the quantity of dross as shown in Figure 49. Similar results were obtained by using zinc chromate primer.

The fact that only the bottom plate surface affected the quantity of dross implies that the mechanism of dross reduction by primer is one of inhibiting adhesion. The primers tested were all "weldable" types, which vaporize cleanly during welding or cutting without leaving residual contaminants. The vaporization of the coating when contacted by molten metal inhibits attachment of the metal as dross. A coating of a non-weldable primer, iron oxide in a linseed oil base, was tried in one test; the quantity of dross was unchanged and the deposit was more difficult to remove. Thus it is not true that the type of primer is not important, although a non-weldable type would seldom be found in an industrial plate shop.

Cuts were also made with primer only on the top surface. No difference in dross formation was seen between primed and non-primed sections. The top-surface primer does, however, affect cutting speed. As seen in the dross curves for 3/4 and l-inch ABS plate (Figures 53 and 54), almost all of the expansion of the dross-free interval is on the low-speed side. Another unusual observation was an almost constant cut squareness. On the 3/4-inch plate, for example, the right-side cut face was square within 2° over the entire dross-free interval. Normally a very wide interval is accompanied by a contour variation vs. speed,

as shown earlier in Figure 20. With primer on the bottom surface only, the cut angle varied 6° over the same range. No effect on speed was seen with the iron-oxide primer.

The presence of zinc primer on the top of the plate apparently reduces heat input from the plasma, especially at the top of the cut. Although the center of the dross curve is shifted to a lower speed, an operating point at its far right can be selected without producing a beveled cut. Thus the practical cutting speed is almost as high as for scaly plate.

The mill scale on unprepared plate surfaces was found to have little effect. Removal of top-surface scale reduced the optimum speed by about 2 ipm when cutting 3/4 inch steel at 400 amps. This difference would be insignificant in everyday operation. A noticeable effect can, however, be induced by selecting an operating point just to the left of the scaly low-speed limit but still above the limit for cleaned plate. An example is shown in Figure 45. Scale was removed from one side of the top surface by grinding. At 400 amperes and 58 ipm, dross was formed on the scaly side only.

The difference between scaly and sandblasted plates was greater when using a larger orifice diameter. As seen in the dross curves for 3/4 and l-inch plate, sandblasting lowered the speed range of the .200 nozzle by roughly 10%. The cause of the higher speed on scaly plate is not known; it is possible that scale boosts speed by adding oxygen to the plasma, but this theory does not explain the increased effect at high current. No speed variation was noticed with the iron-oxide primer, but the thickness and oxide content of the primer are less than those for mill scale.

Sandblasting of the bottom plate surface neither promoted nor inhibited the occurrence of dross, but dross removal was made easier. The deposit on a sandblasted plate was always less tenacious than a similar quantity on uncleaned plate. The rough "peak-and-valley" profile of a sandblasted surface undoubtedly inhibits wetting of the plate by the molten dross; the high surface tension of a liquid metal will not allow the metal to penetrate the valleys. This theory is supported by the experiment shown in Figure 57. A section of sandblasted 3/4-inch plate was fine-ground to a surface finish of approximately 32 micro-inches roughness. When cuts were made at 400 amperes and 60 ipm, dross appeared on the smooth bottom surface; removal required the use of a hammer and chisel. It appeared-that the smooth and relatively clean surface aided wetting by the liquid metal. Figure 57 also illustrates the tendency, when operating in a narrow dross-free interval, for dross formation to continue once started by a fluctuation in conditions. A lighter dross can be seen on the sandblasted surfaces at the ends of the cuts.

6.9 Conclusions and Operating Guidelines .

The following summary serves as a guide for achieving maximum cut quality on mild steel.

(1) The best way to select the proper speed and current for cutting an unfamiliar material is to generate a dross curve. The optimum cut contour will then be achieved near the midpoint of the dross-free interval.

(2) If a dross-free operating range cannot be found, the conditions should be selected to give low-speed dross rather than high-speed. Dross removal will be easier and loss of cut will be avoided.

(3) In general an increase in current, while staying within the nozzle's capacity, will expand the dross-free interval.

(4) For plate thicknesses near the transition between recommended orifice diameters, the use of the larger orifice will give improved quality at higher speed. The same technique can be used on plate of slightly smaller thickness, at the expense of some rounding of the top edge. A typical application for this approach is high-speed ripping where best edge squareness is not a requirement.

(5) Normal errors in gas flow are unlikely to be the cause of a dross problem. Incorrect gas flow can, however, be a symptom of defective torch components, which will be accompanied by poor performance.

(6) The flow of "cut water" in a water injection torch is important; a minimum flow is necessary to avoid dross. A slightly high flow is preferable to a low one, -although too much cut water reduces electrode life.

(7) Torch-to-work distance (standoff) must be controlled for best results. The appearance of patches of dross in a long cut, accompanied by non-uniform cut angle, suggests a varying standoff.

(8) Pre-coating of the plate with a weldable primer will significantly reduce dross formation. The use of zinc-base primers will require a slight reduction in cutting speed for an optimum cut, although quite acceptable quality is obtained without this adjustment. In the event that cutting is to be done on plate with only one primed surface, that surface sholud be placed on the bottom.

(9) Sandblasting of plate surfaces requires no change in operating conditions in most cases. The most noticeable effect will be greater ease of dross removal if dross is formed.

FIGURES

and

TABLES

Table I

SUGGESTED CONDITIONS
FOR WATER INJECTION CUTTING

Thickness Inches	Nozzle Orifice	Gas Flow (CFH)	Cut Water Flow (GPM)	Speed (IPM)	Current (AMPS)
CARBON AND STAINLESS STEEL:					
1/4				140	300
1/2	.156	140	.33	90	350
1				30	400
1				60	575
1-1/2	.200	180	.40	35	600
2				20	600
2				30	700
	.230	220	.48		
3				15	750
ALUMINUM:					
1/4				160	300
1/2	.156	140	.33	110	350
1				50	400
1				90	550
1-1/2	.200	180	.40	45	600
2				35	600
2				50	650
	.230	220	.48		
3				30	750

Table II

ARC LENGTHS WHEN WELDING FOILS*

Process	Arc Length, In.	Tolerance, In.
Needle Arc	1/4	± 1/16
Gas tungsten-arc	0.025	± 0.005

*Welding done at 10 amps dcsp or less.

Table III

MANUAL NEEDLE ARC WELDING BUTT JOINTS IN FOILS AND THIN SHEET[a]

Thickness, In.	Welding Current amp, dcsp	Speed, ipm	Shielding Gash
Stainless Steel			
0.001l[c]	0.3	5	Argon-1% H_2
0.003[c]	1.6	6	Argon-1% H_2
0.005C	2.4	5	Argon-1% H_2
0.010	6	8	Argon-1% H_2
0.020	15	10	Argon
0.020	17	24	Argon-5% H_2
0.030	10	3	Argon
0.030	10	5	Argon-1% H_2
0.030	17	10	Argon-5% H_2
0.050	13	4	Argon-5% H_2
0.062	17	3	Argon-10% H_2
Titanium			
0.003[c]	3	6	Argon
0.008	5	6	Argon
0.015	8	5	Argon
0.022	12	9	Helium-25% A
Inconel 718			
0.012	6	15	Argon-1% H_2
0.016	3.5	6	Argon-1% H_2
Hastelloy X			
0. 005[c]	4.8	10	Argon-1% H_2
0.010	5.8	8	Argon-1% H_2
0.020	10	10	Argon-1% H_2
Copper			
0.003[c]	10	6	Helium-25% A

[a]Argon flow rate - 0.5 CFH through a 0.030 in. dia. nozzle.
[b]Shielding gas flow - 20 CFH.
[c]Flanged butt joint.

Table IV

OPERATING CONDITIONS/KEYHOLE MODE

Plate Thickness (in.)	Welding Speed (ipm)	Arc Current (amp)	Nozzle Diameter (in.)	Orifice Gas Flow (CFH)	Gas Type	
					Orifice	Shield
Mild Steel						
1/8	12	185	.111	13	Ar	CO_2
3/16	10	220	.136	12	Ar	CO_2
1/4	14	275	.136	15	Ar	CO_2
Stainless Steel						
3/32	38	160	.111	5	95%Ar-5%H_2	Ar
1/8	24	145	.111	10	95%Ar-5%H_2	Ar
3/16	16	165	.136	12	95%Ar-5%H_2	Ar
1/4	14	240	.136	18	95%Ar-5%H_2	Ar
Titanium						
1/8	19	185	.111	8	Ar	Ar
3/16	13	175	.136	18	Ar	Ar
1/4	12	200	.136	22	50%Ar-50%He	Ar
1/2	10	275	.136	27	50%Ar-50%He	Ar

Text Reference	C	ppm O	S	P	Mn	Si	Ni	Cr	Mo	Cu	V	Ti	Al
3/4" 1018	.20	215	.032	.010	.58	.047	.16	.11	.020	.37	.002	.003	<.005
1" 1018	.19	205	.030	.010	.61	.034	.13	.09	.017	.22	.002	.003	<.005
3/8" 1022	.19	104	.017	.008	.72	.030	.027	.017	.013	.019	.002	.002	<.005
1/2" 1022	.19	122	.018	.008	.96	.030	<.02	.017	.013	.018	.002	.002	<.005
3/4" 1022	.18	137	.026	.008	1.18	.030	<.02	.019	.013	.011	.060	.002	<.005
5/8" Danish 42, Iron oxide primer	.12		.045	.020	.50	.22	.10	.084	.014	.25	.002	.002	<.005
5/8" Scaly ABS	.19	101	.023	.008	.96	.024	<.02	.018	.010	<.02	.002	.003	<.005
5/8" S.B. ABS	.19	98	.023	.008	.98	.026	<.02	.018	.009	<.02	.002	.003	<.005
5/8" primed ABS	.23	102	.036	.010	.99	.024	<.02	.020	.010	.011	.002	.002	<.005
3/4" Scaly ABS	.13	18	.021	.007	.67	.15	<.02	.018	.008	.035	.002	.003	.026
3/4" S.B. ABS	.13	12	.021	.008	.60	.13	<.02	.017	.008	.032	.002	.003	.031
3/4" primed ABS	.13	13	.022	.010	.63	.17	<.02	.021	.009	.040	.002	.003	.040
1" S.B. ABS	.17	109	.018	.010	.83	.028	<.02	.017	.009	<.02	.002	.003	.006
1" primed ABS	.19	82	.019	.010	.87	.026	<.02	.017	.009	.015	.002	.003	<.005

Notes: (1) Steels referred to as 1018 and 1022 in text differ primarily in Mn content.

(2) All values in percent by weight, except oxygen (ppm).

(3) 1-inch scaly and 1/2-inch ABS plates were not analyzed.

S.B. = Sandblasted

Table V. CHEMICAL ANALYSES OF PLATES USED

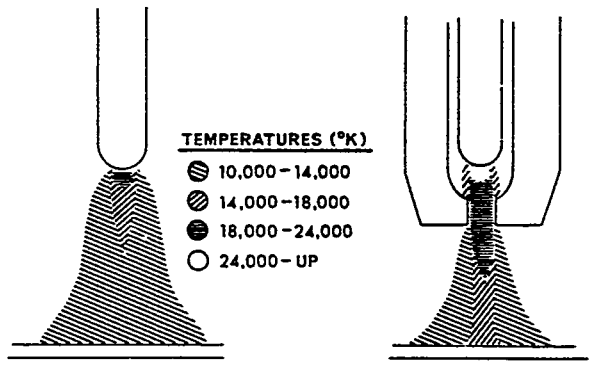

FIGURE 1. TEMPERATURE DIFFERENCES.

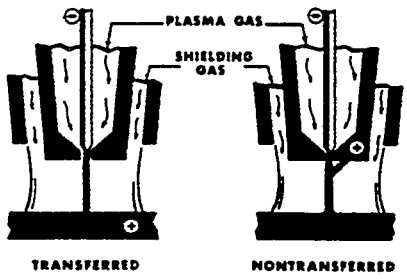

FIGURE 2. TWO BASIC TYPES OF CONSTRICTED ARCS.

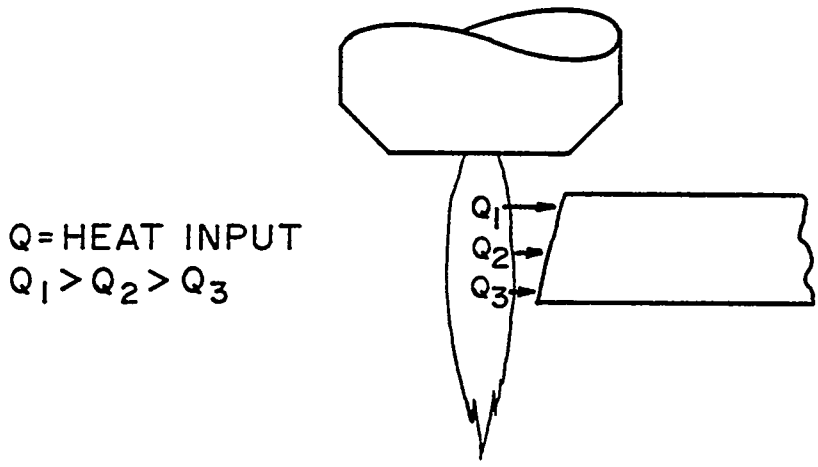

FIGURE 3. POSITIVE CUT ANGLE.

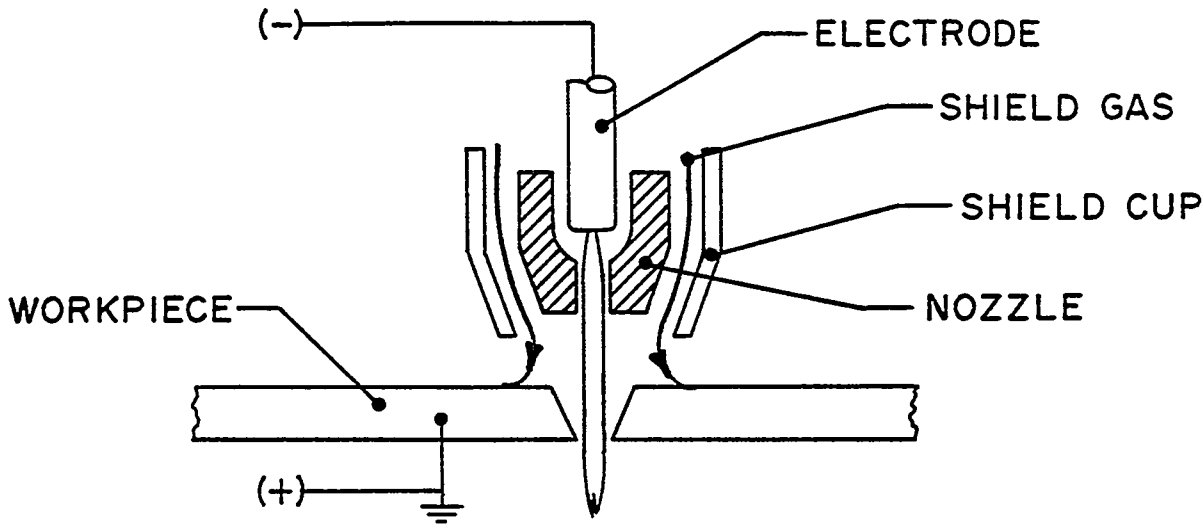

FIGURE 4. DUAL FLOW TECHNIQUE.

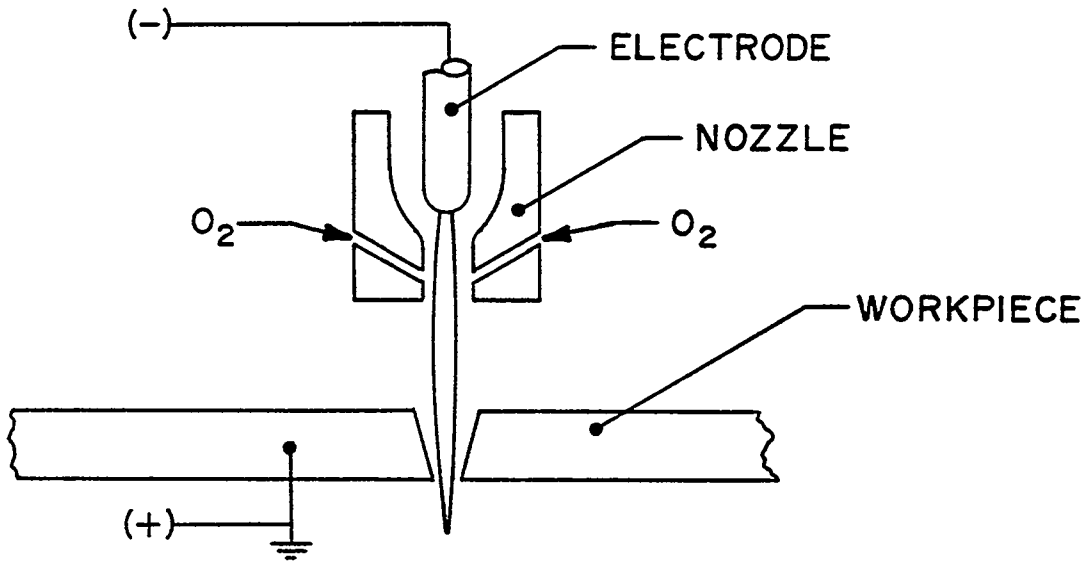

FIGURE 5. OXYGEN INJECTION TECHNIQUE.

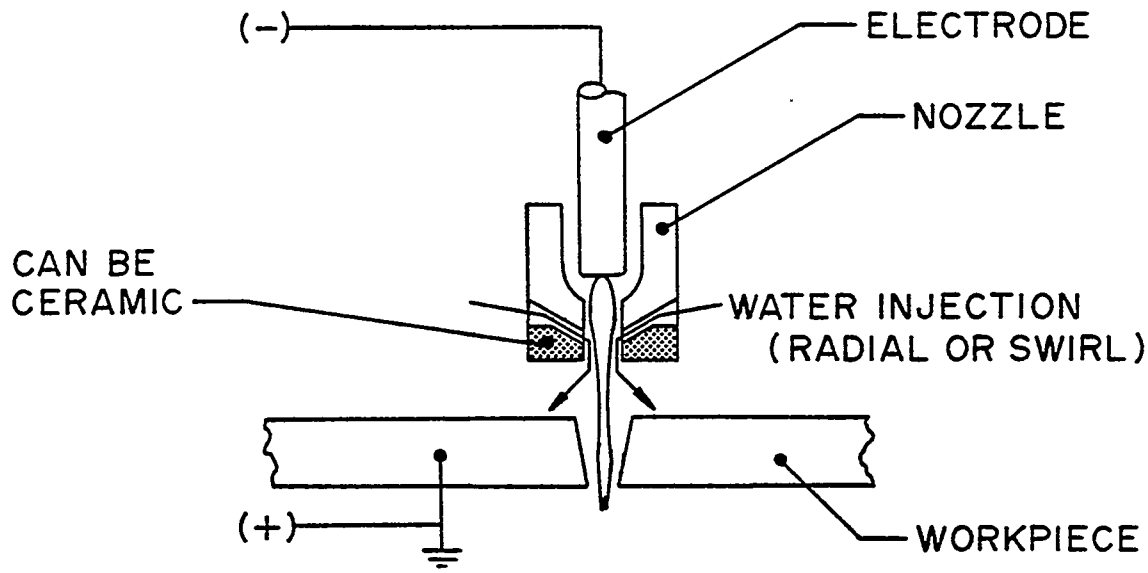

FIGURE 6. WATER INJECTION TECHNIQUE.

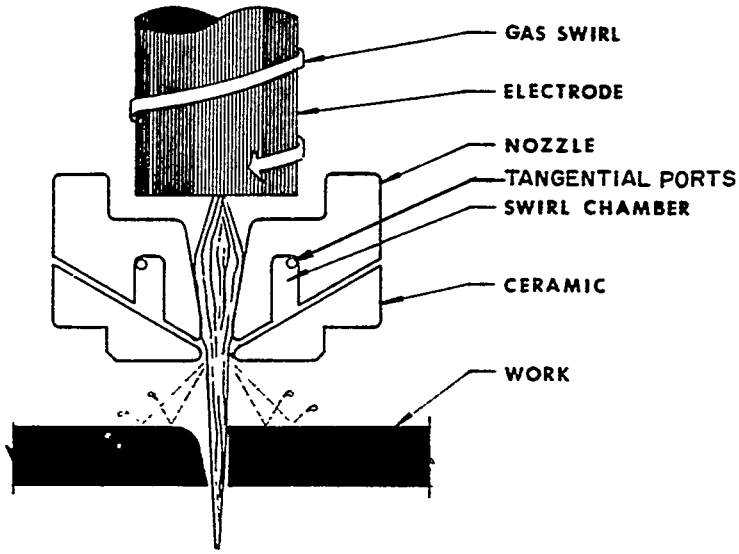

FIGURE 7. SWIRL INJECTION NOZZLE.

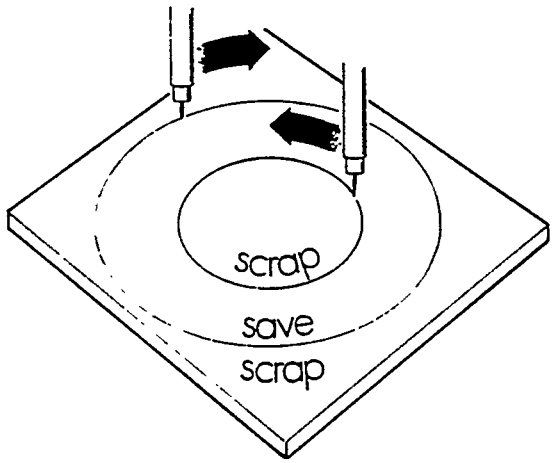

FIGURE 8. DIRECTION OF CUT.

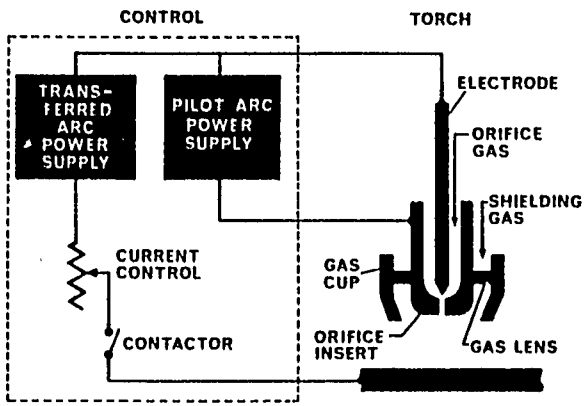

FIGURE 9. NEEDLE ARC SYSTEM SCHEMATIC.

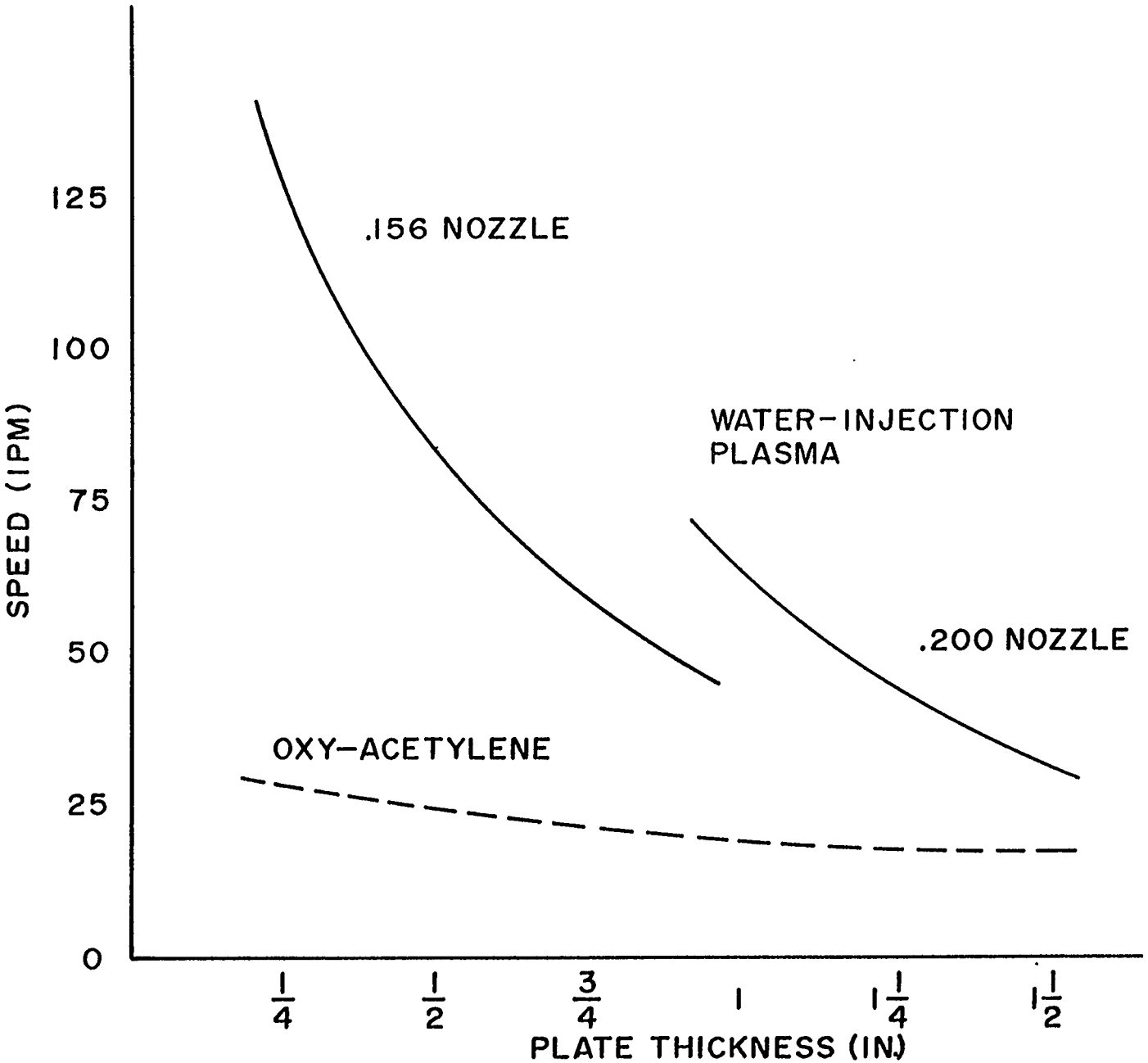

FIGURE 10. TYPICAL CUTTING SPEEDS.

SINGLE TORCH

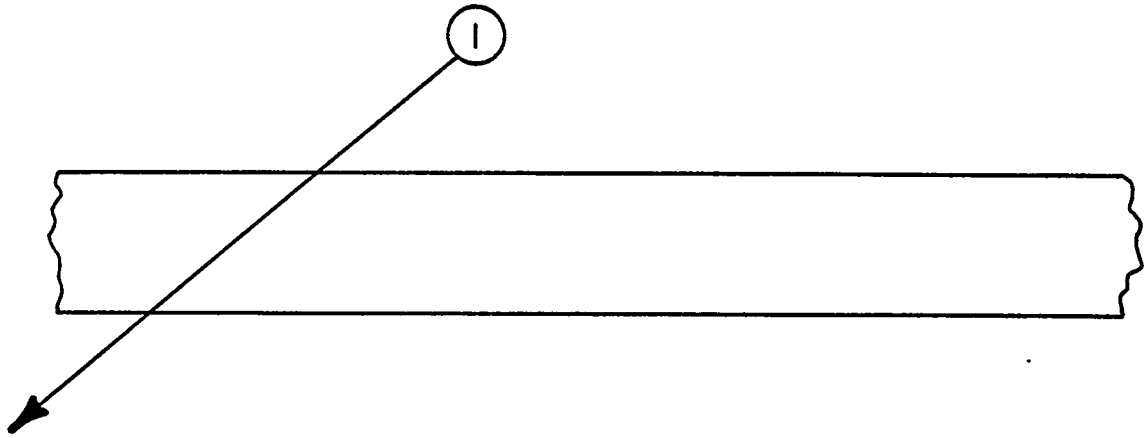

DOUBLE TORCH

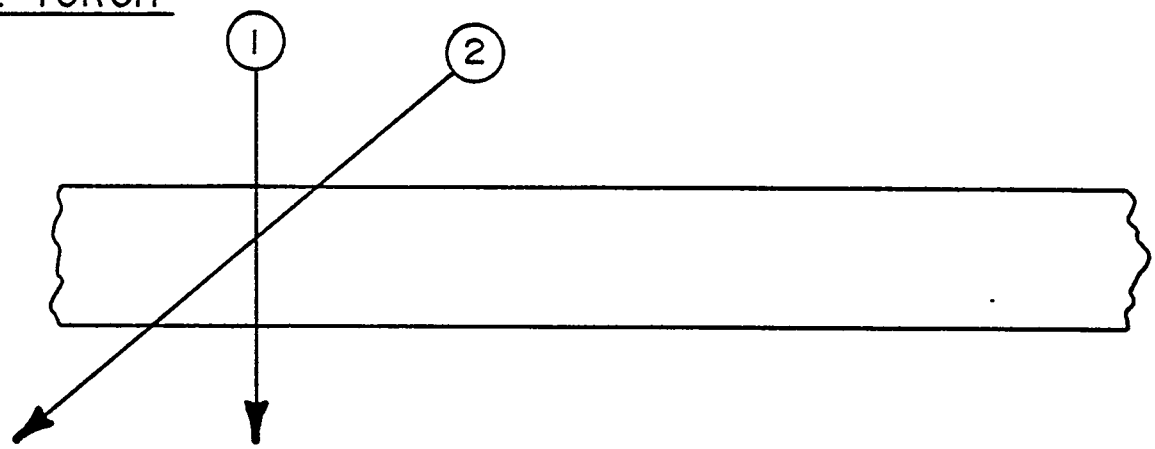

TRIPLE TORCH

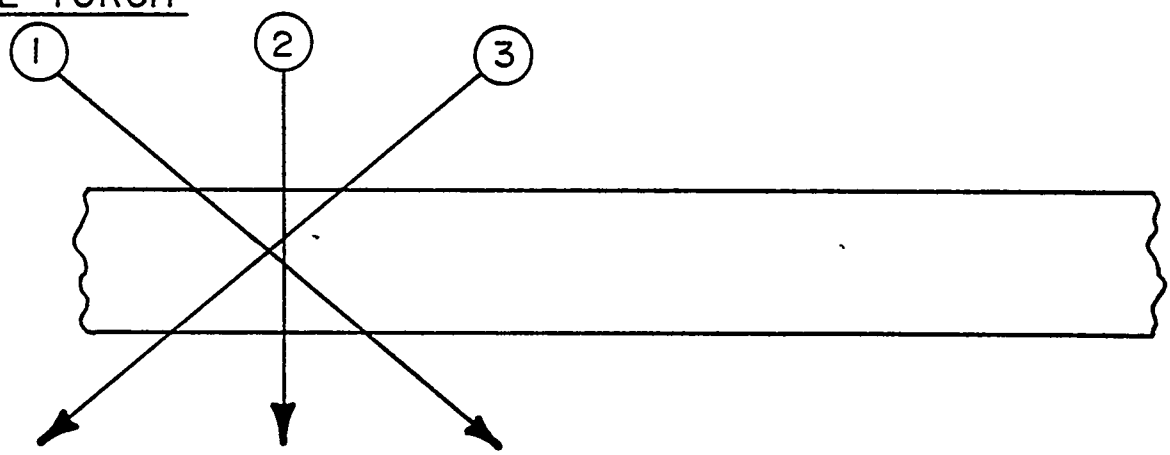

FIGURE 11. TORCH SEQUENCE FOR BEVELING.

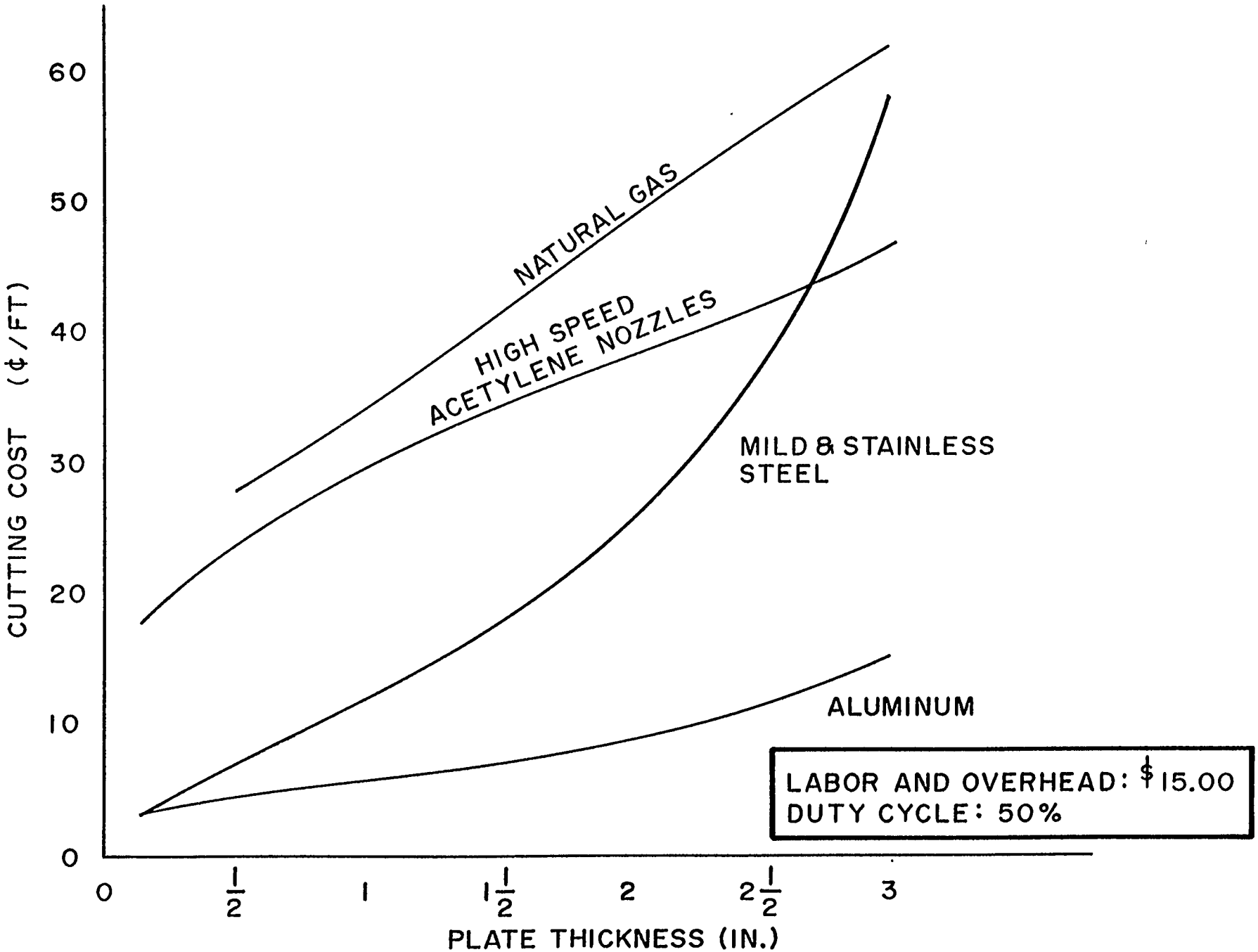

FIGURE 12. TYPICAL CUTTING COSTS.

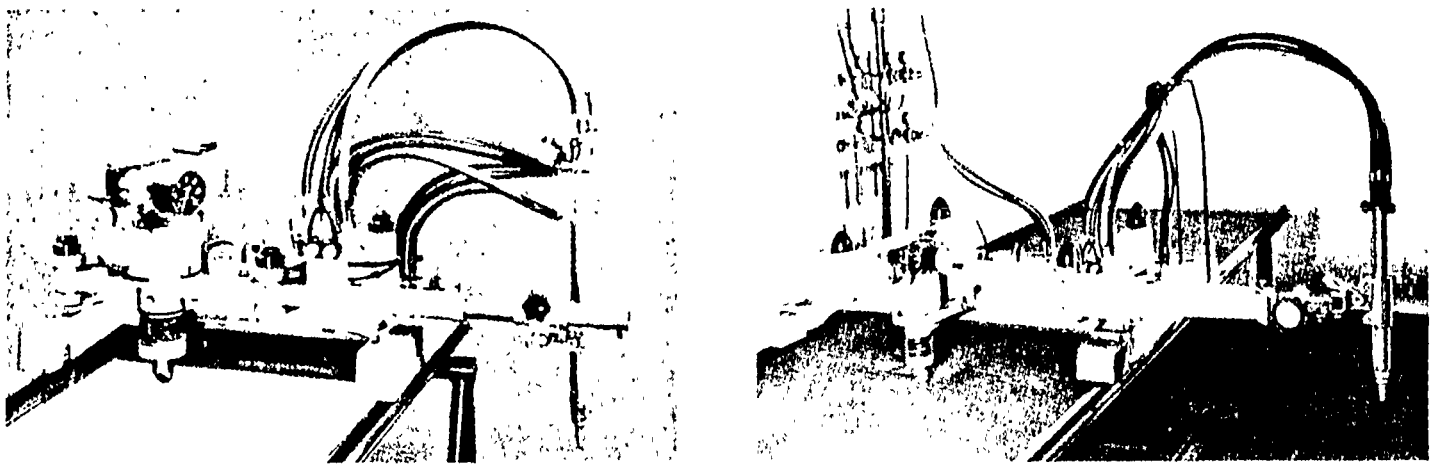

FIGURE 13. EARLY PANTOGRAPH MACHINES (CM-15-18 AND CM-15-36).

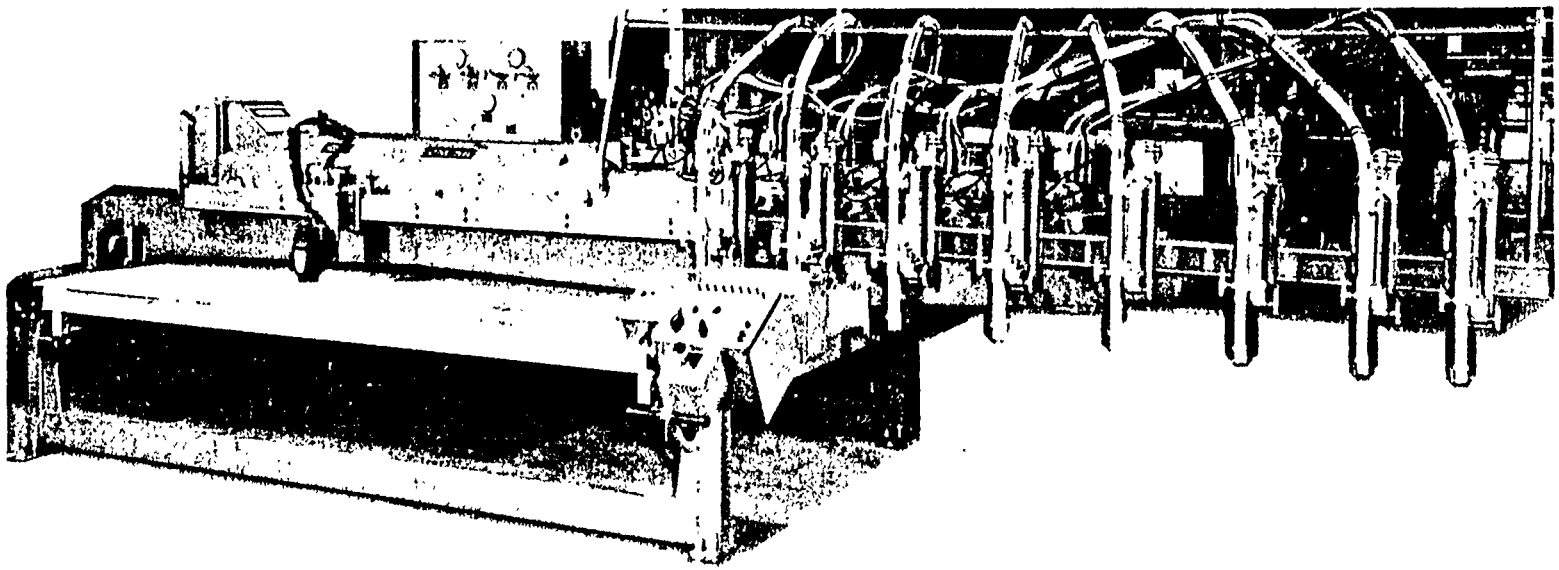

FIGURE 14. Coordinate Drive Gas Cutting Machine (CM-56), 1962. Cantilever Construction.

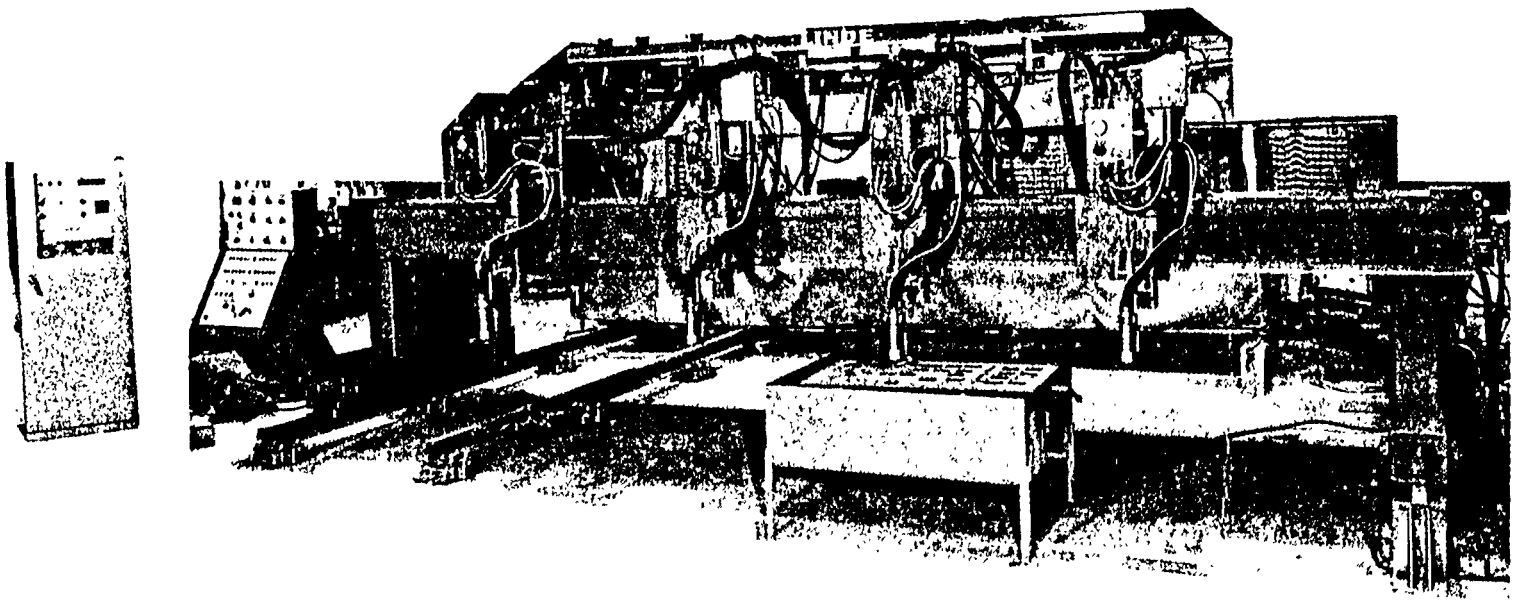

FIGURE 15 Four-Plasma Cutting Machine in Lab, 1974 (CM-100). Bridge Construction. Numerical Control at Left.

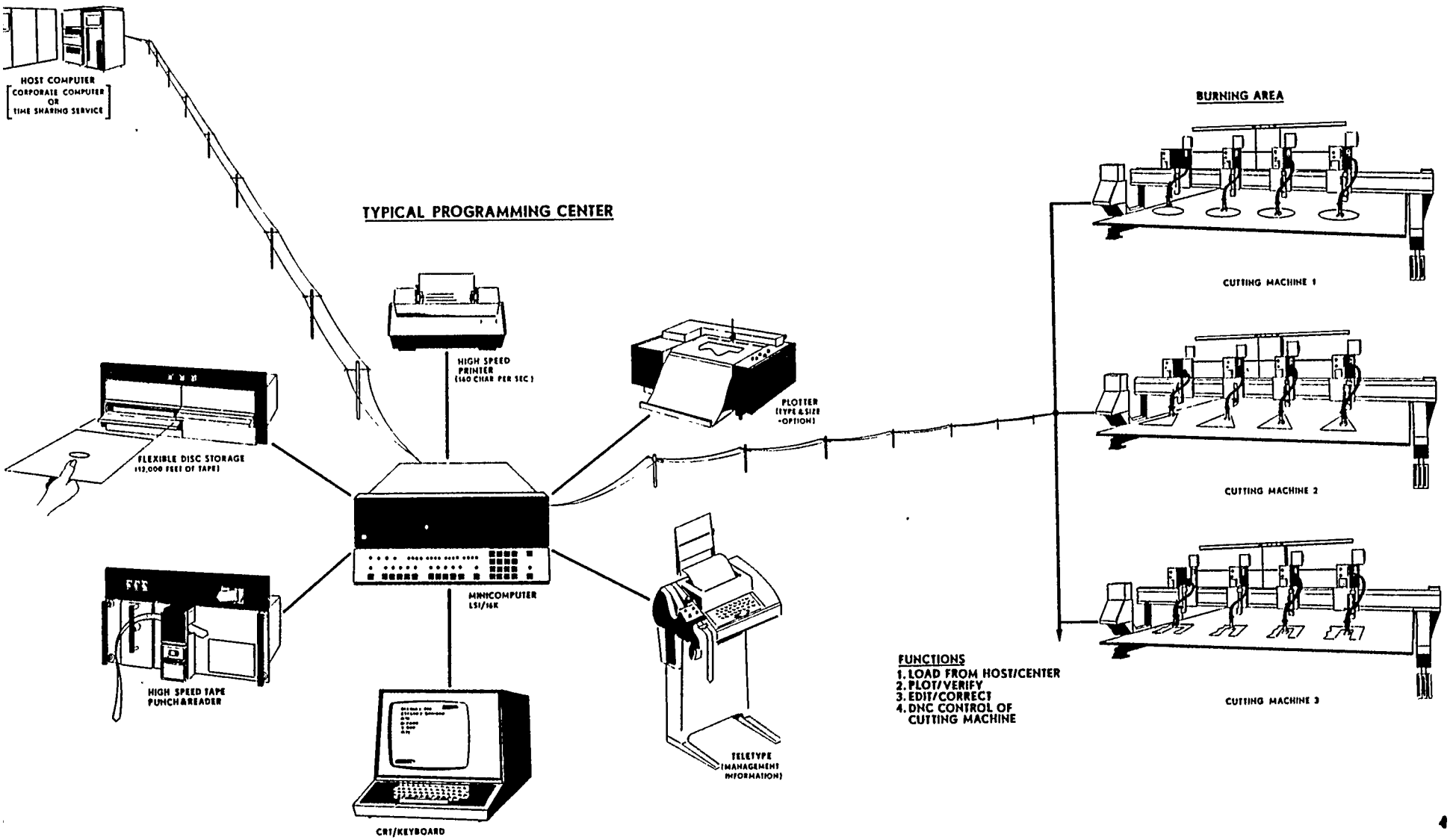

FIGURE 16. DIRECT NUMERICAL CONTROL

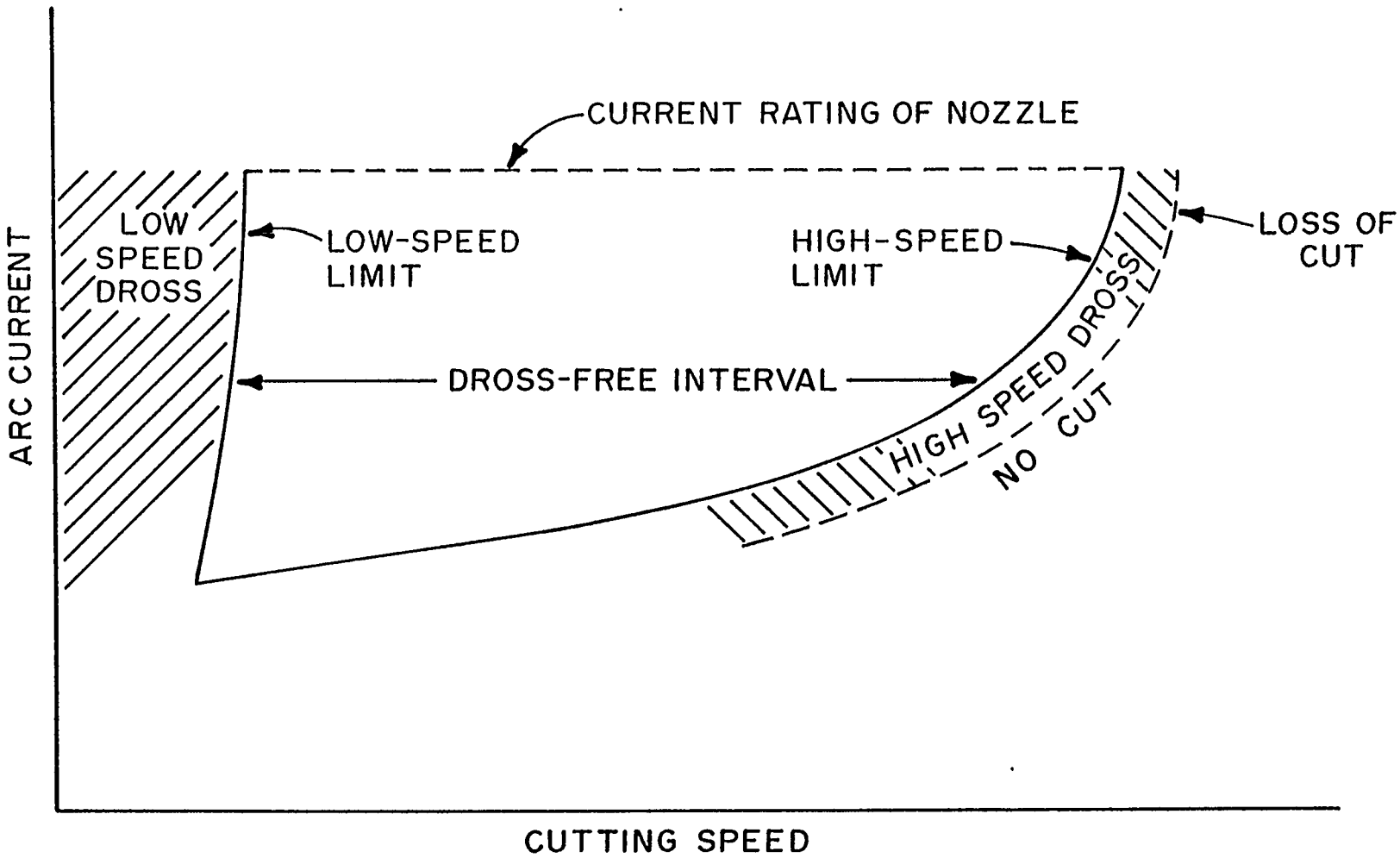

FIGURE 17. SCHEMATIC DROSS CURVE.

CUTTING CHARACTERISTICS OF A 5X12 -52WA NOZZLE ON 1/2 INCH 304 STAINLESS STEEL.

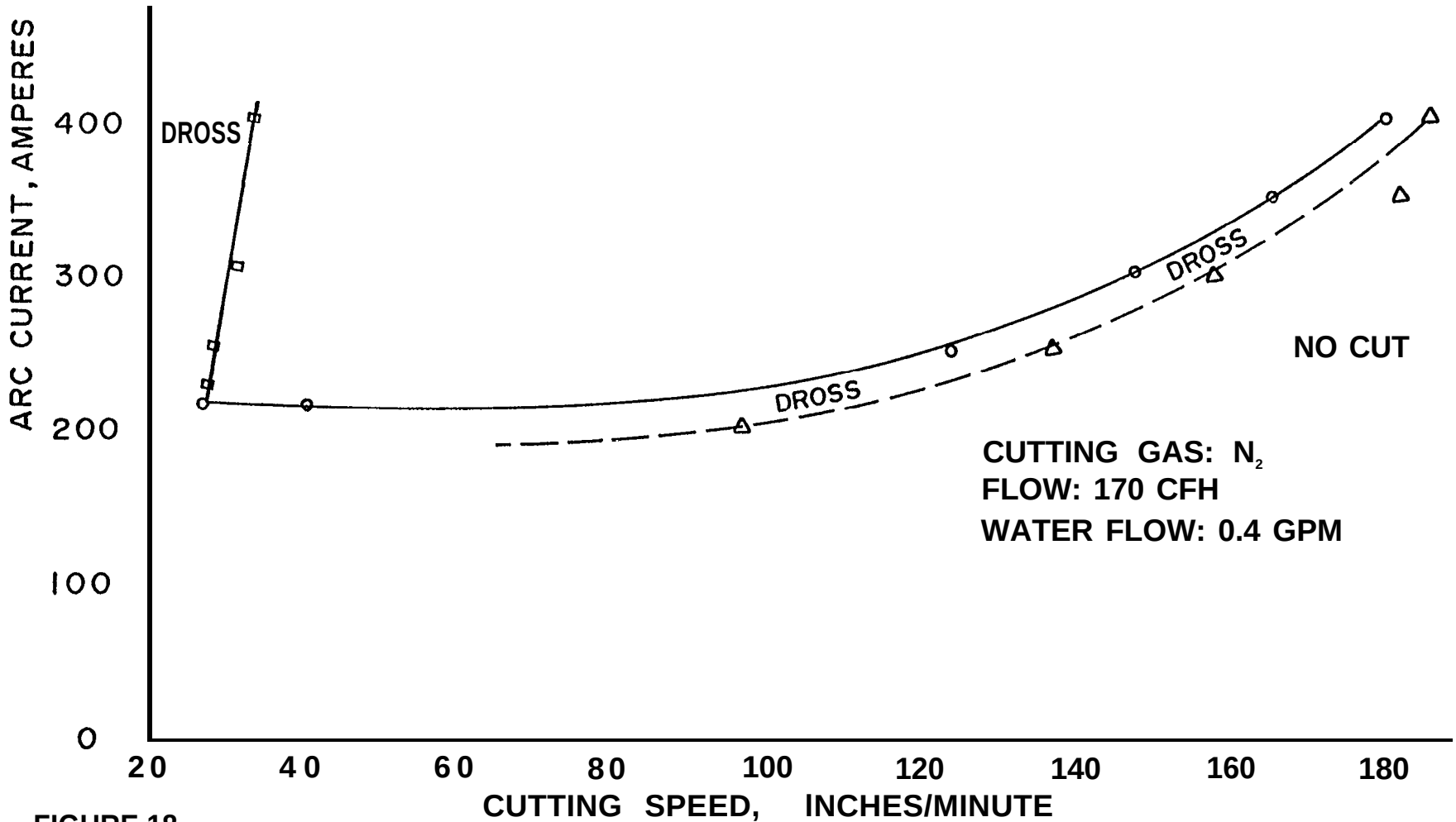

FIGURE 18.

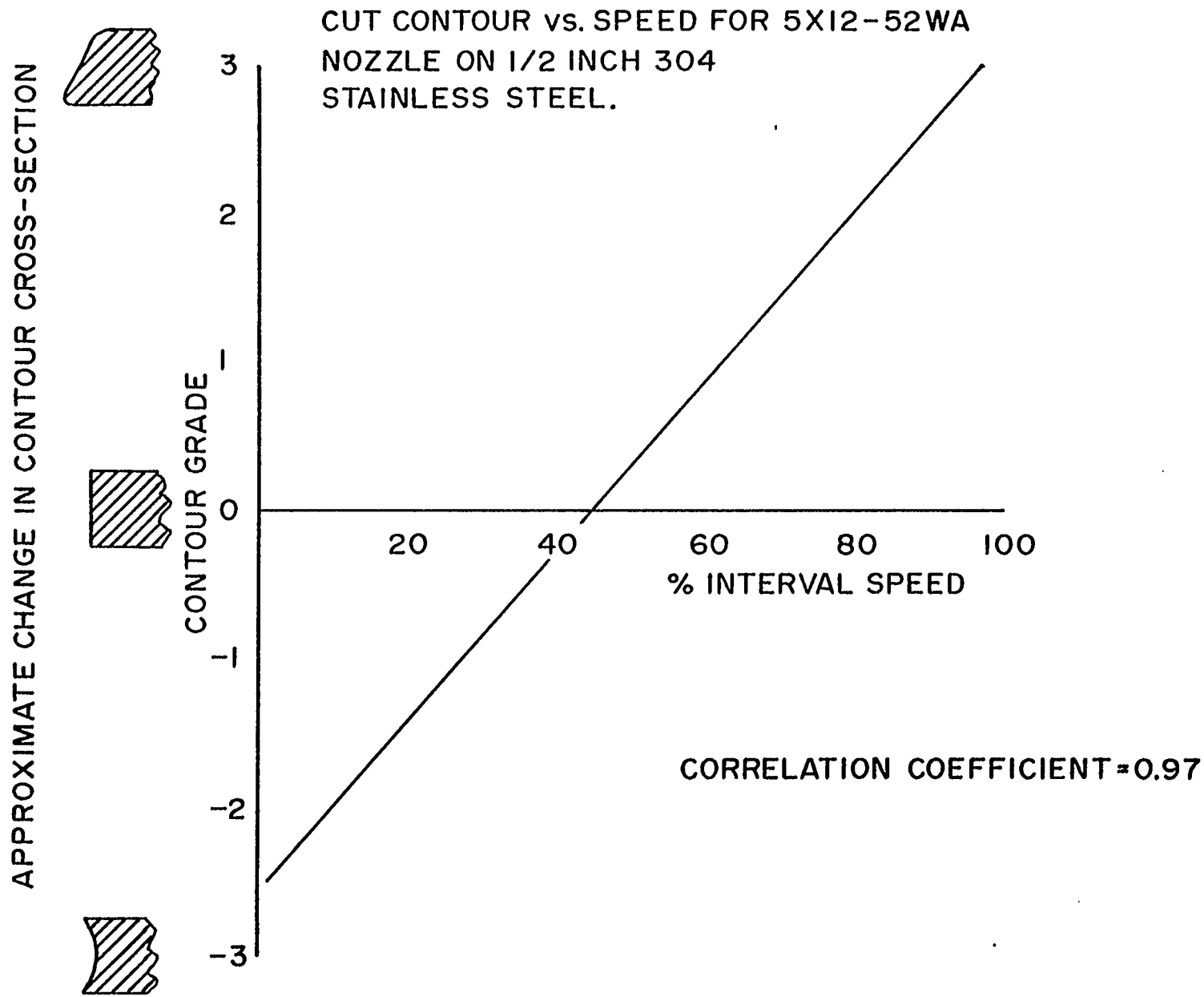
CUT CONTOUR vs. SPEED FOR 5X12-52WA
NOZZLE ON 1/2 INCH 304
STAINLESS STEEL.
APPROXIMATE CHANGE IN CONTOUR CROSS-SECTION
CONTOUR GRADE
3
2
1
0
-1
-2
-3
20
40
60
80
100
% INTERVAL SPEED
CORRELATION COEFFICIENT = 0.97

FIGURE 19.

OPTIMUM OPERATING RANGE FOR 5 X 12-52WA NOZZLE ON $\frac{1}{2}$" 304 STAINLESS STEEL.

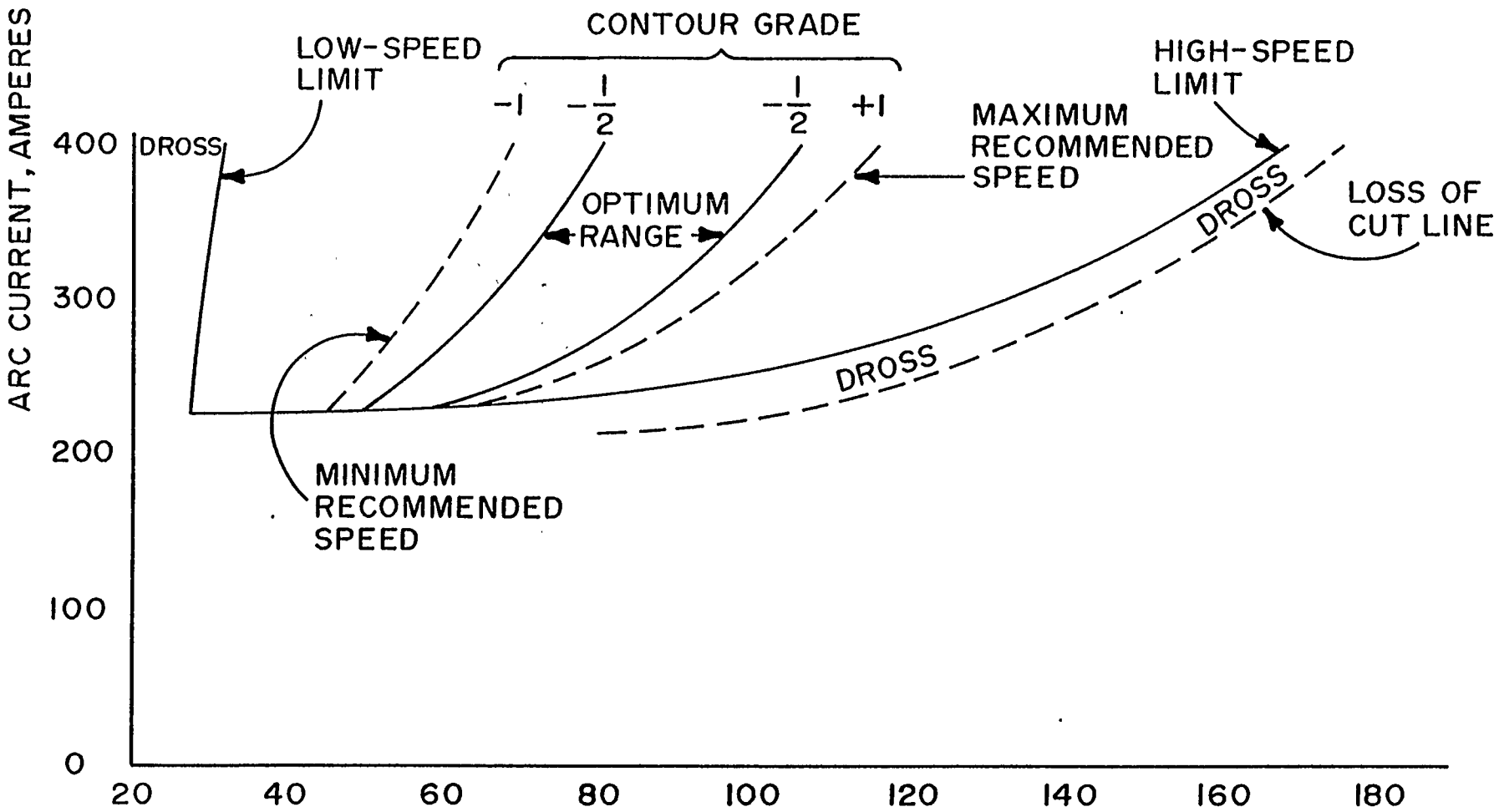

FIGURE 20.

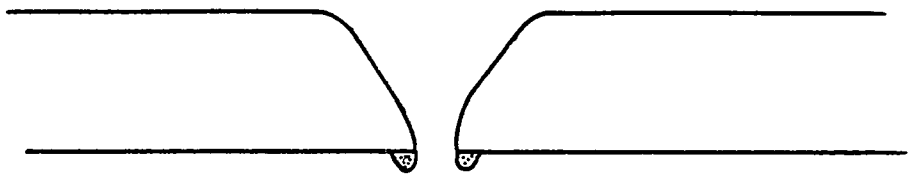

HIGH SPEED

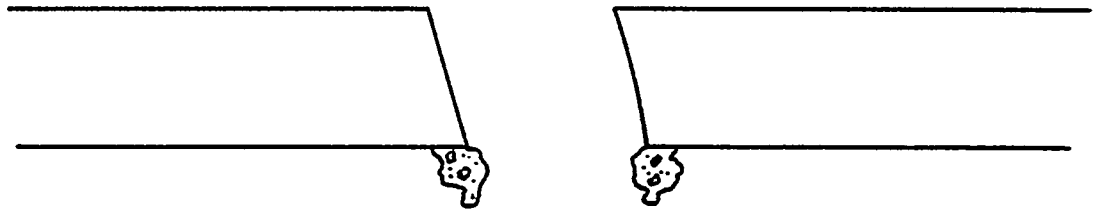

LOW SPEED

FIGURE 21. SCHEMATIC CUT QUALITY AT EXTREME SPEEDS.

(1.6X)

FIGURE 22. LOW SPEED DROSS.

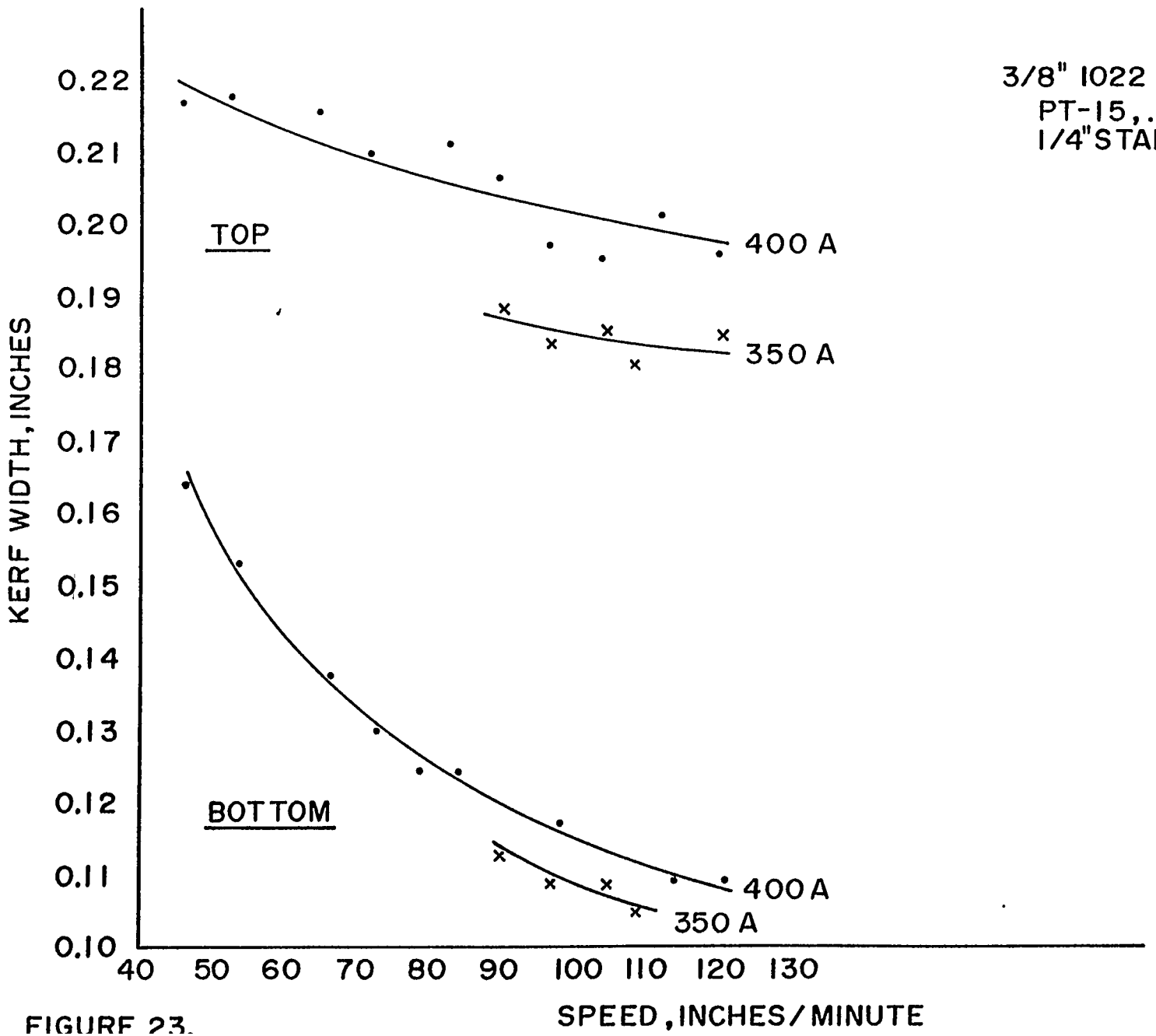
3/8" 1022 STEEL
PT-15, .156 NOZZLE
1/4" STANDOFF
TOP
400 A
350 A
BOTTOM
400 A
350 A
KERF WIDTH, INCHES
0.22
0.21
0.20
0.19
0.18
0.17
0.16
0.15
0.14
0.13
0.12
0.11
0.10
40
50
60
70
80
90
100
110
120
130
SPEED, INCHES/MINUTE

FIGURE 23.

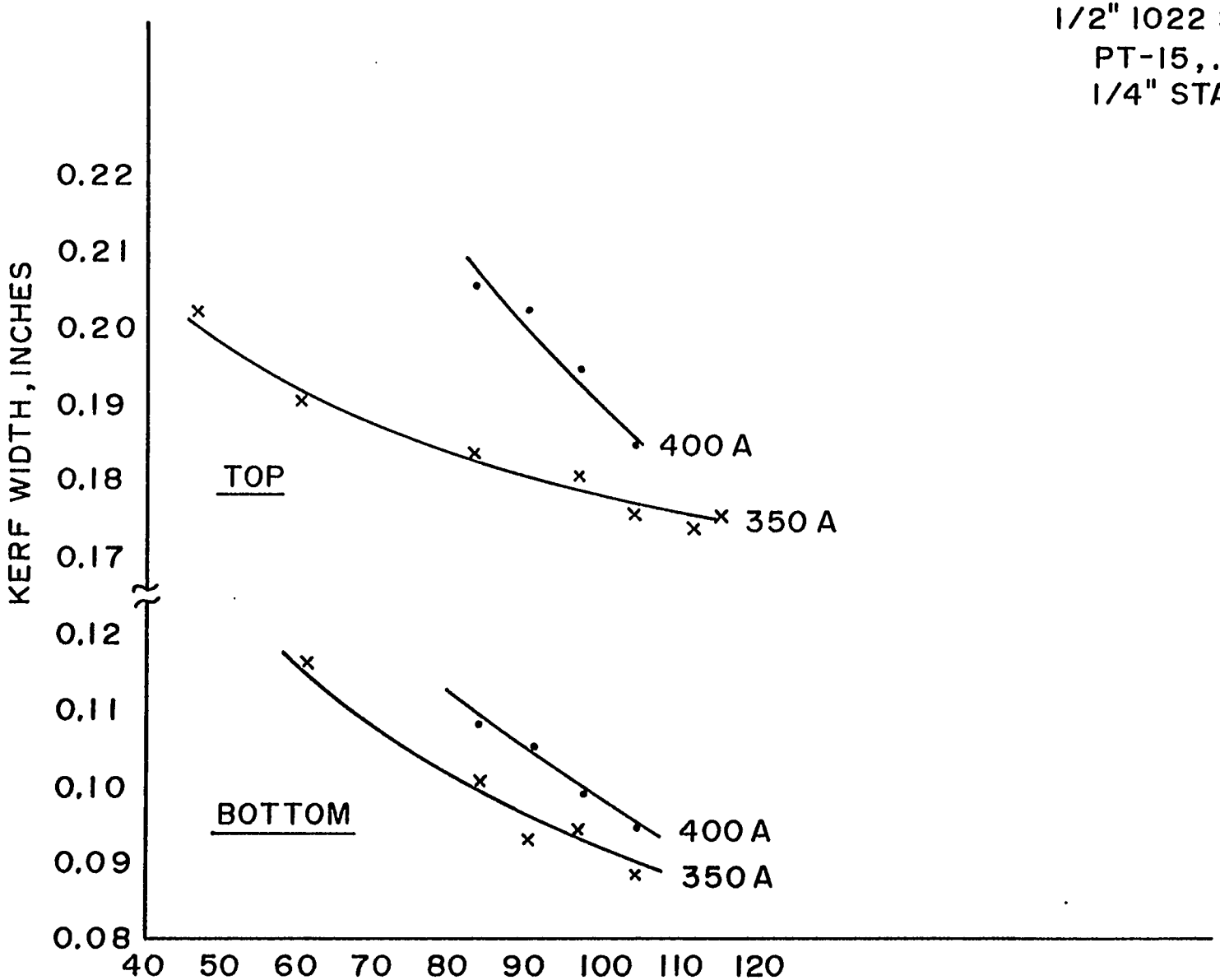
1/2" 1022 STEEL
PT-15, .156 NOZZLE
1/4" STANDOFF
KERF WIDTH, INCHES
0.22
0.21
0.20
0.19
0.18
0.17
0.12
0.11
0.10
0.09
0.08
TOP
400 A
350 A
BOTTOM
400 A
350 A
40 50 60 70 80 90 100 110 120
SPEED, INCHES/MINUTE

FIGURE 24.

3/4" 1022 STEEL
PT-15, .156 NOZZLE
1/4" STANDOFF
400 AMPERES

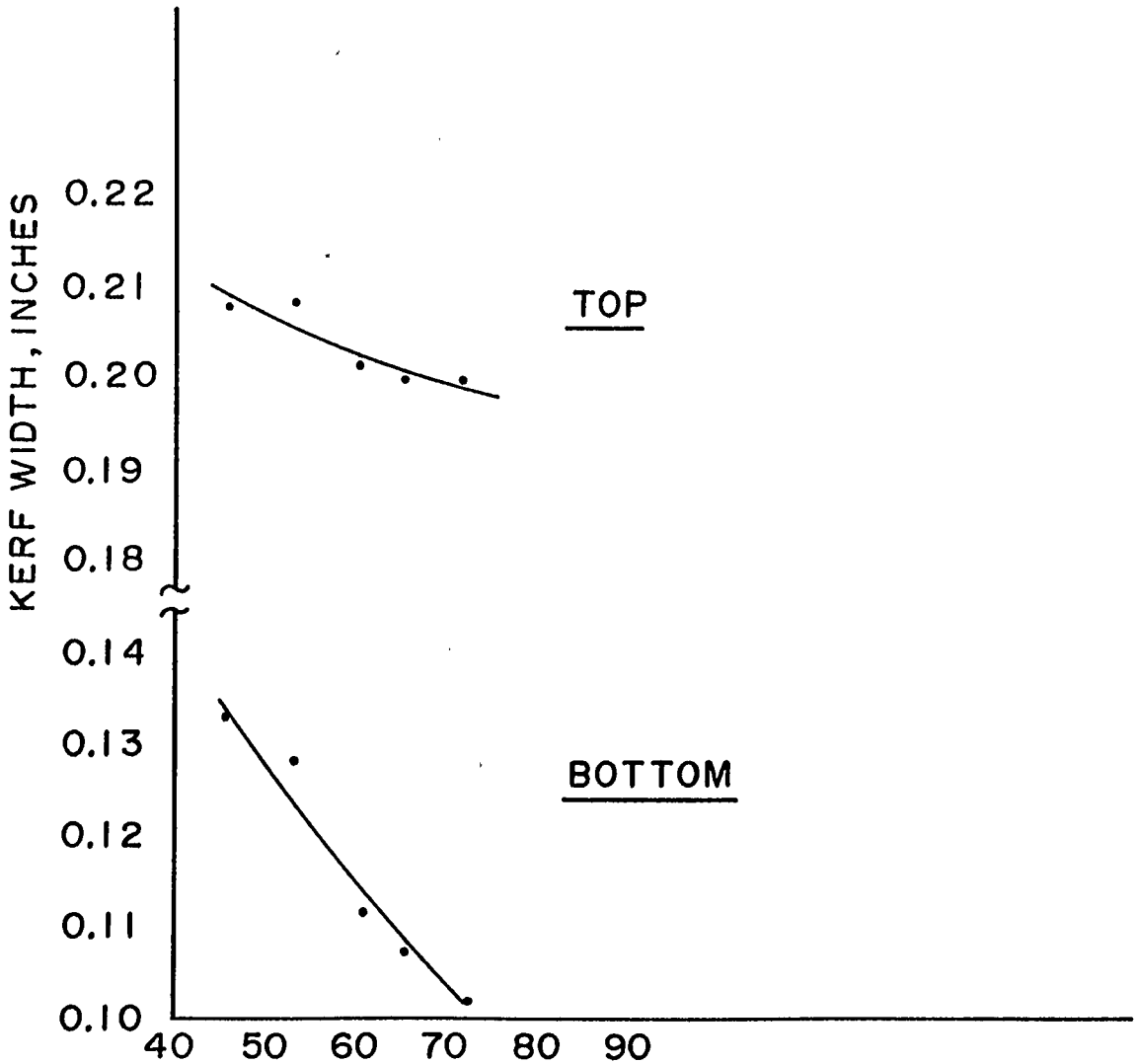

FIGURE 25.

(IX)

FIGURE 26. HIGH SPEED DROSS AND LOSS OF CUT.

(IX)

FIGURE 27. DROSS AT HIGH AND LOW SPEED LIMITS (BOTTOM VIEW) 3/4" 1018 STEEL, 400 AMPS, TOP 63 IPM, BOTTOM 65 1PM.

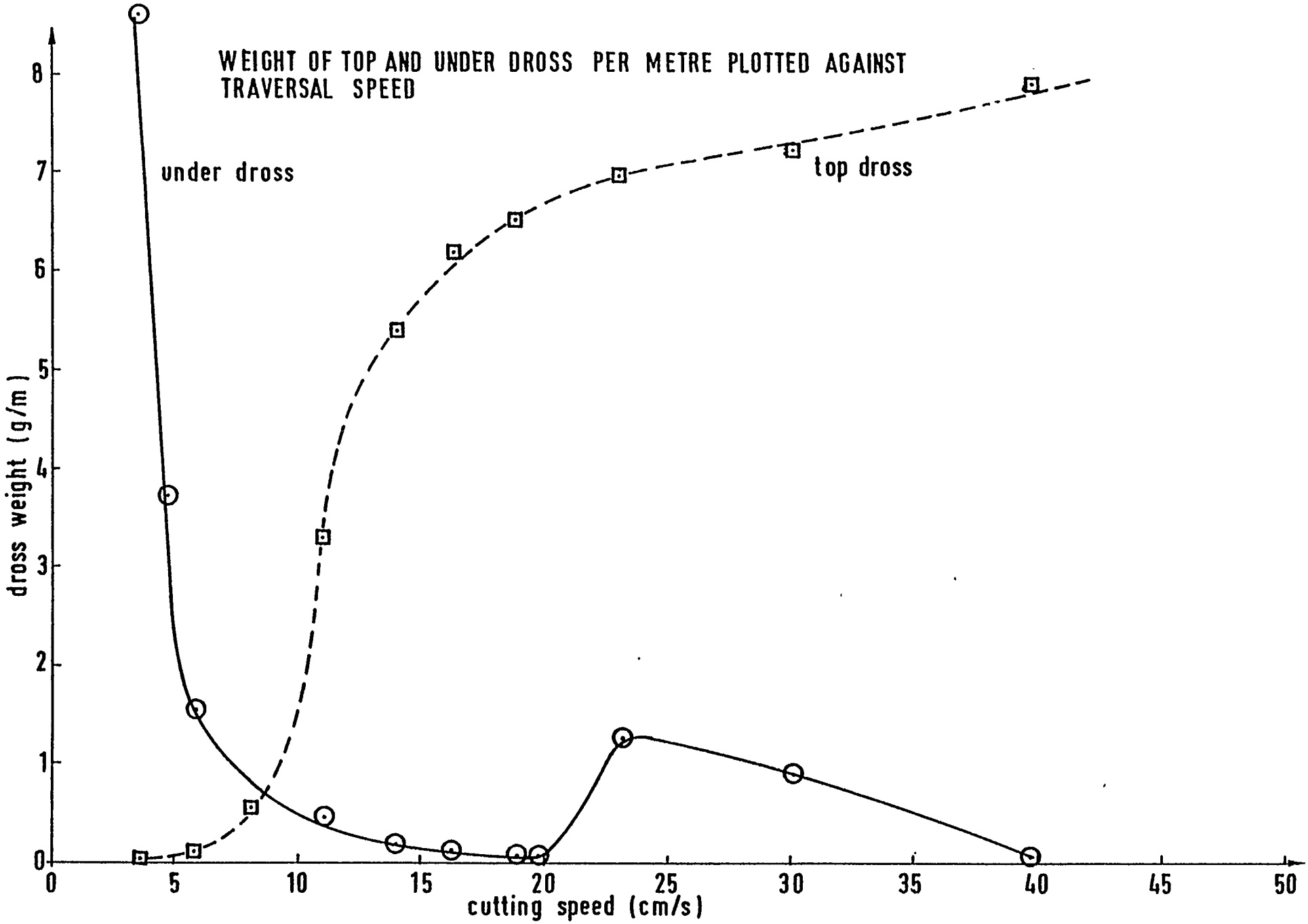
WEIGHT OF TOP AND UNDER DROSS PER METRE PLOTTED AGAINST TRAVERSAL SPEED
under dross
top dross
dross weight (g/m)
cutting speed (cm/s)
0
1
2
3
4
5
6
7
8
0
5
10
15
20
25
30
35
40
45
50

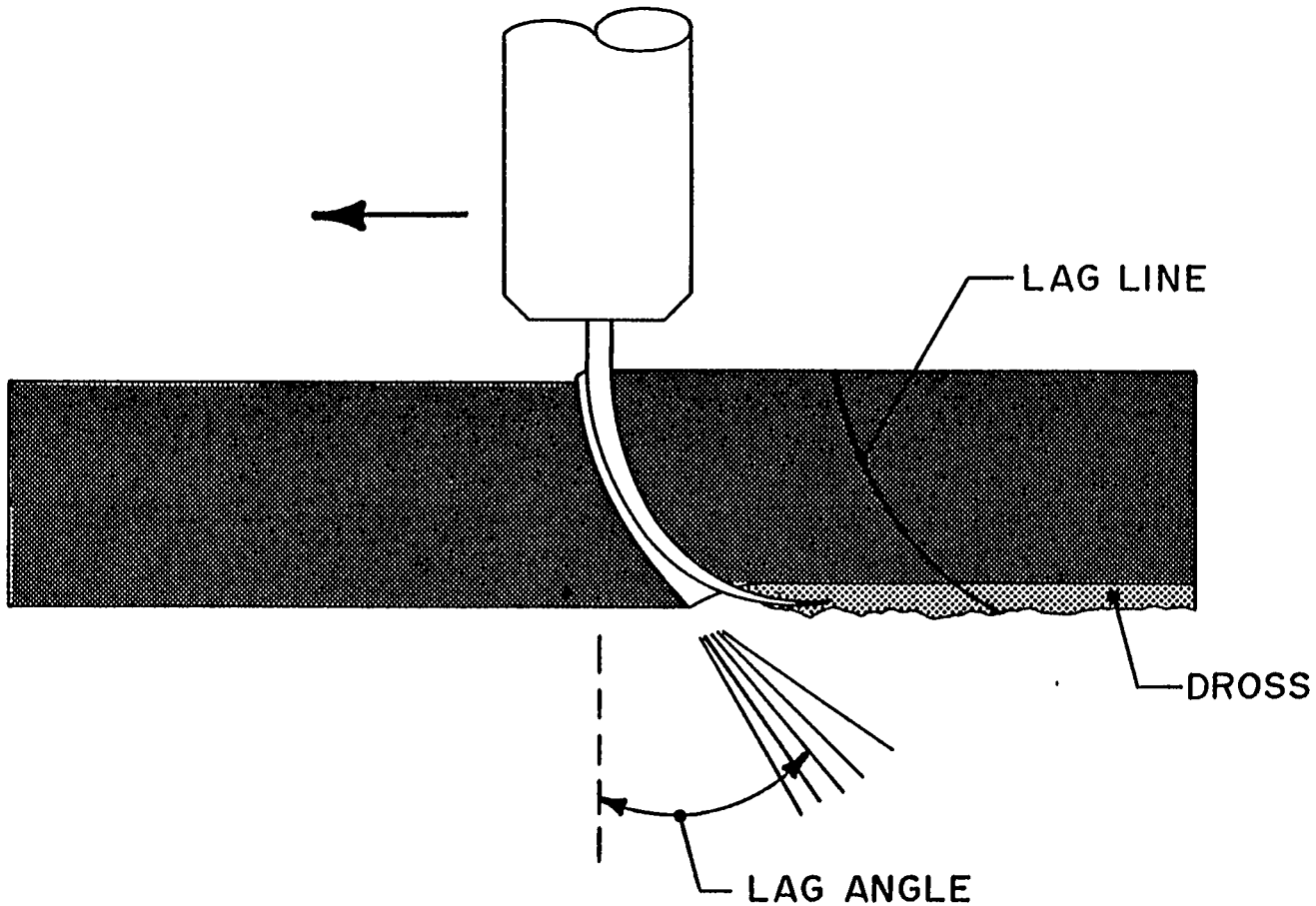

FIGURE 29. HIGH-SPEED CUTTING.

3/8" 1022 STEEL
PT-15,156 NOZZLE
375 AMPERES
1/4" STANDOFF
140 CFH N_2

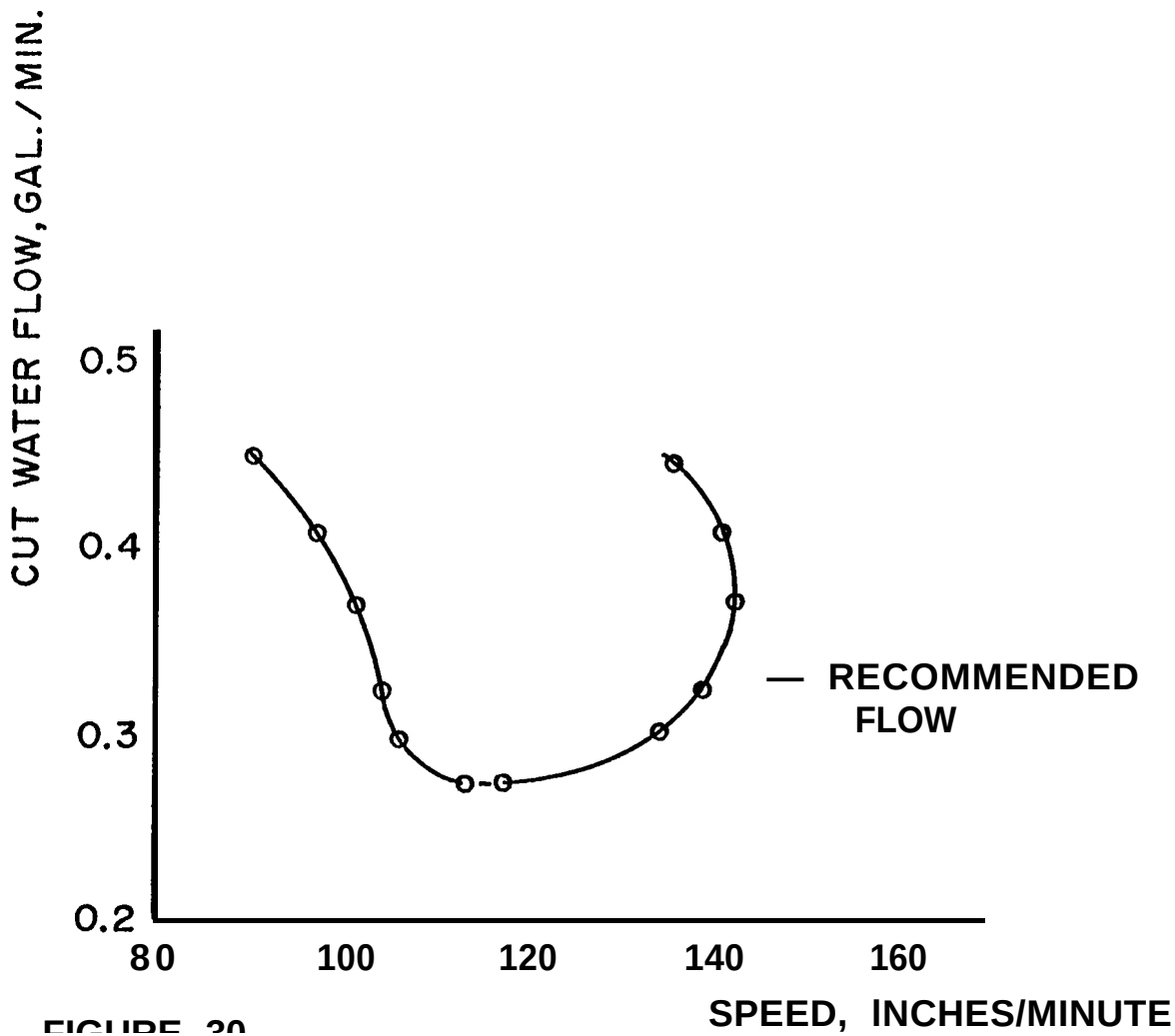

FIGURE 30

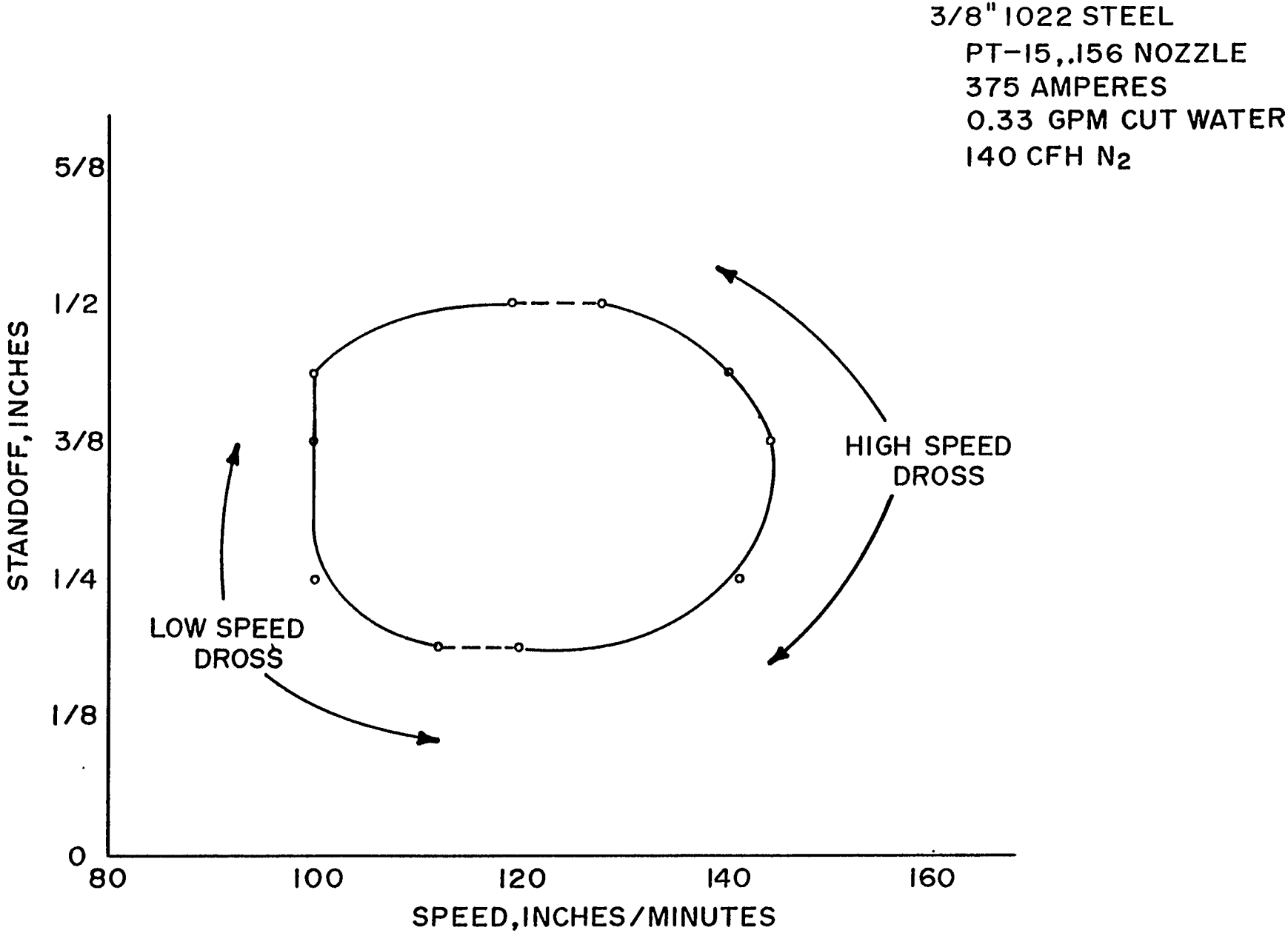

FIGURE 31. DROSS LIMITS vs STANDOFF

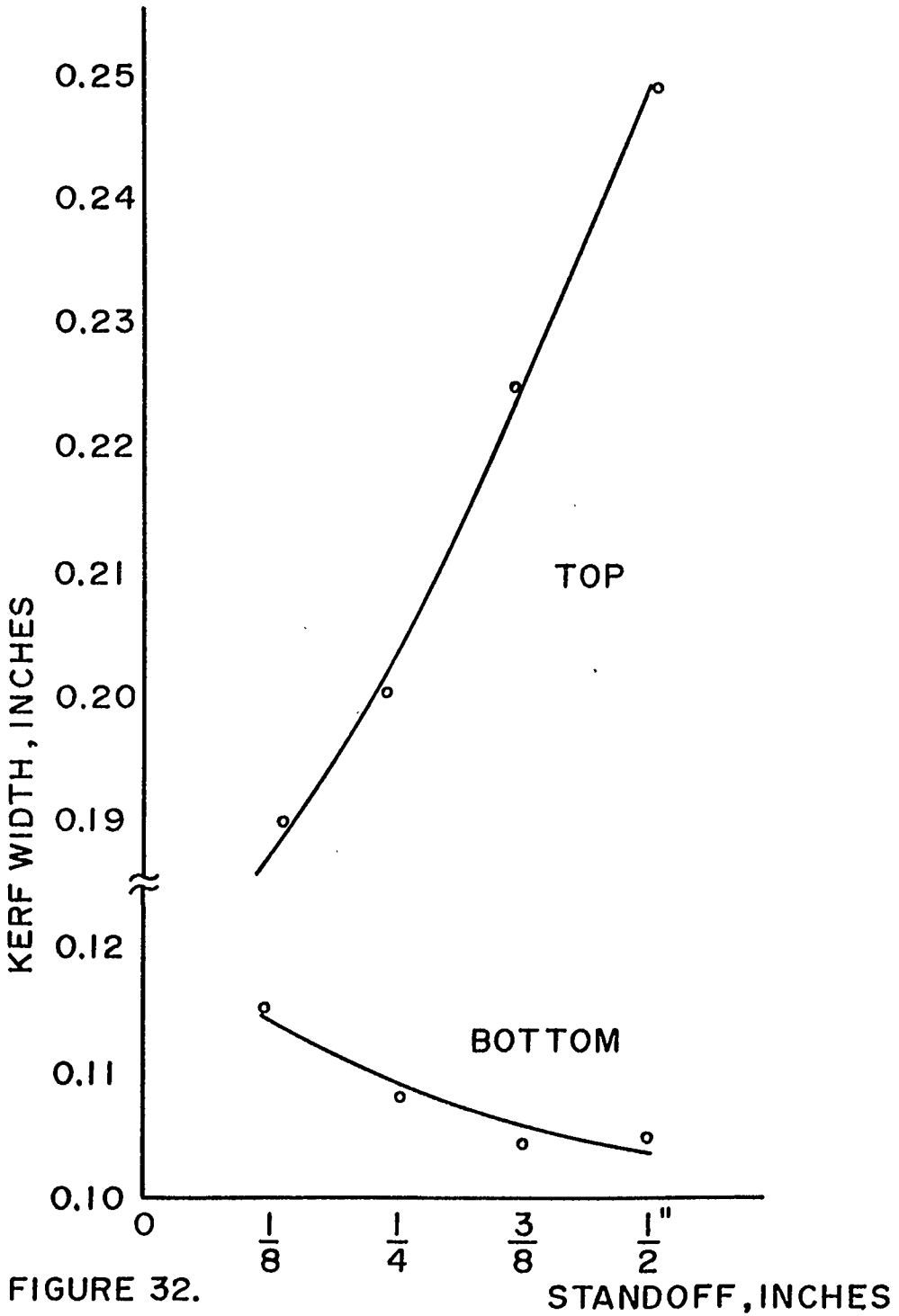

3/8" 1022 STEEL
PT-15, .156 NOZZLE
400 AMPERES
112 IPM

FIGURE 32.

(1.2X)

FIGURE 33.

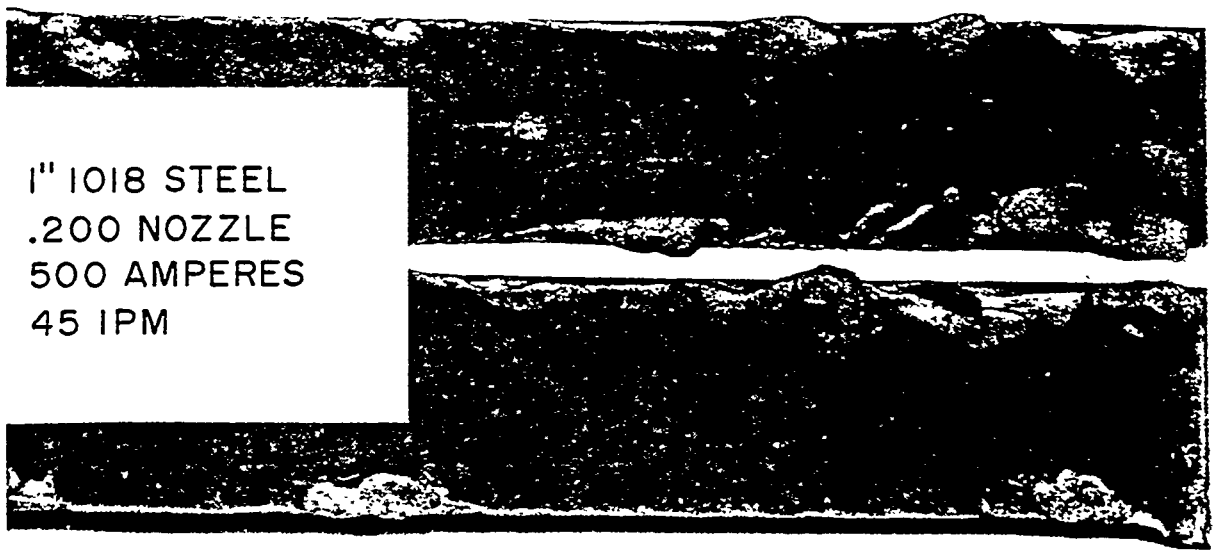

(1.2X)

FIGURE 34.

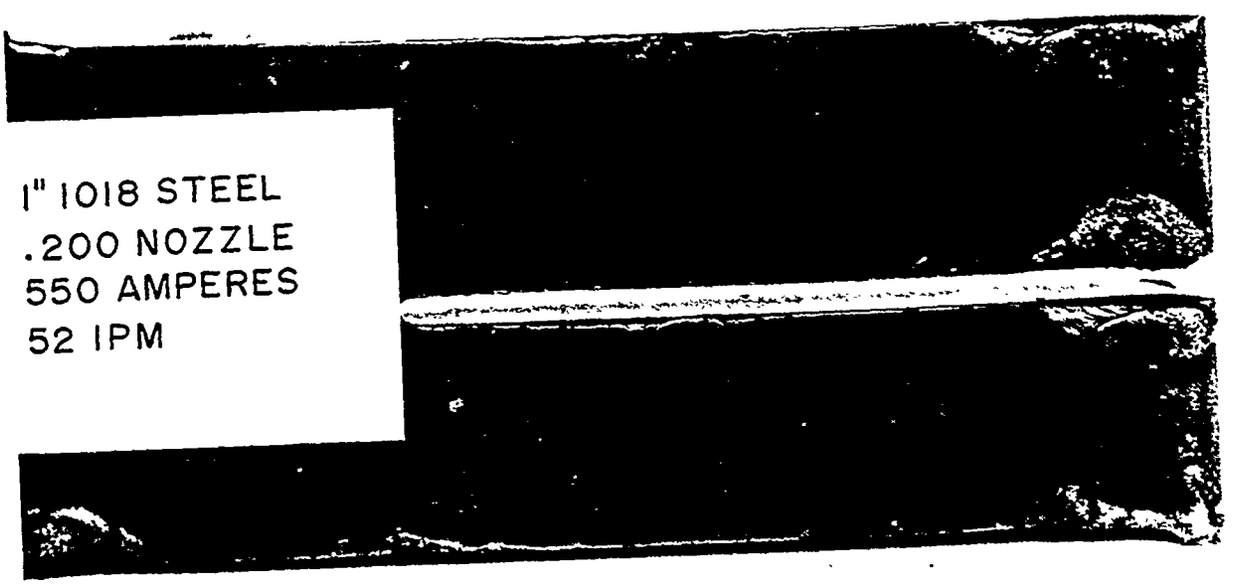

(1.2X)

FIGURE 35.

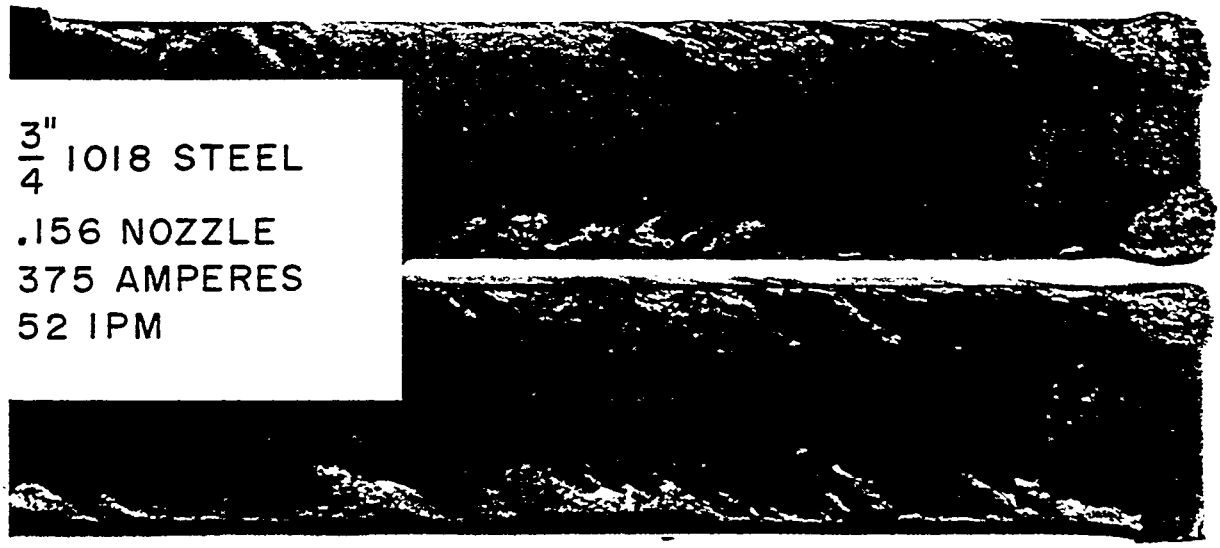

(1.2X)

FIGURE 36.

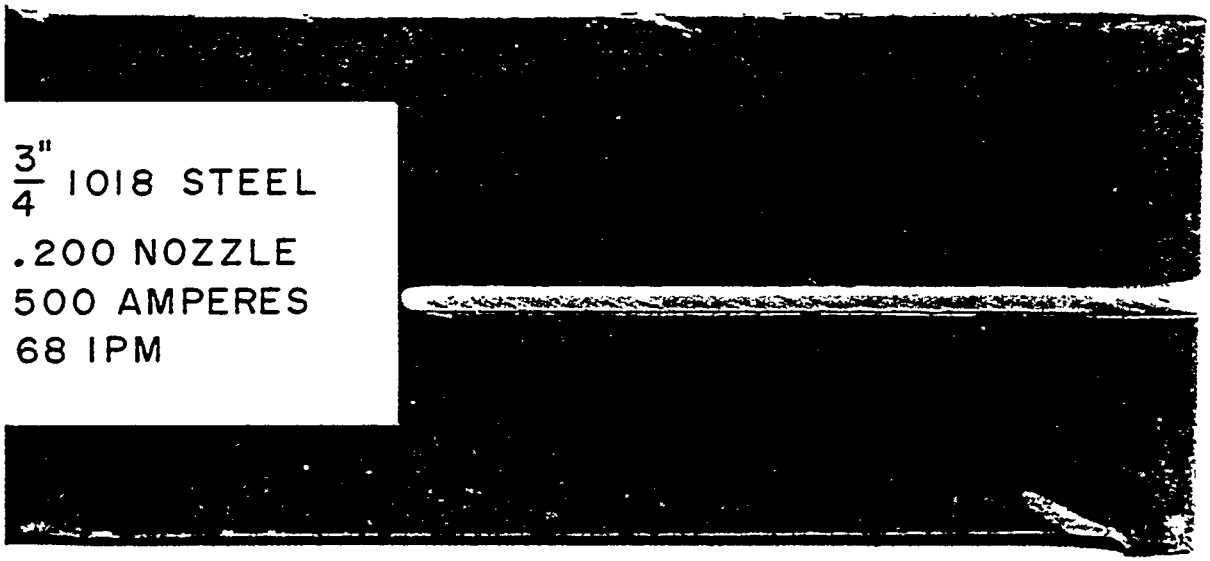

(1.2X)

FIGURE 37.

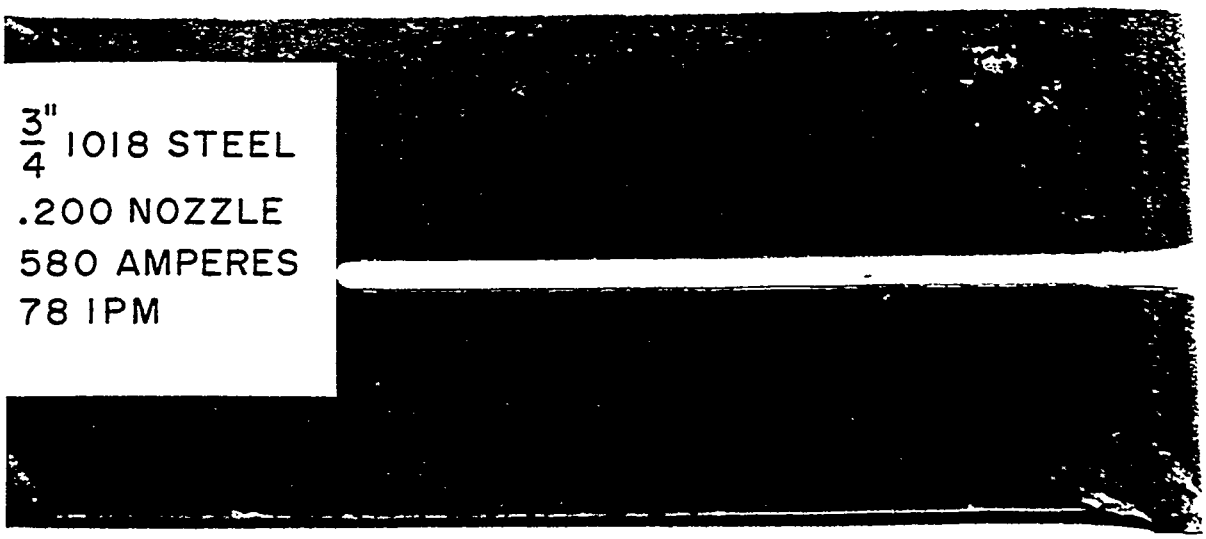

(1.2X)

FIGURE 38.

LEFT SIDE

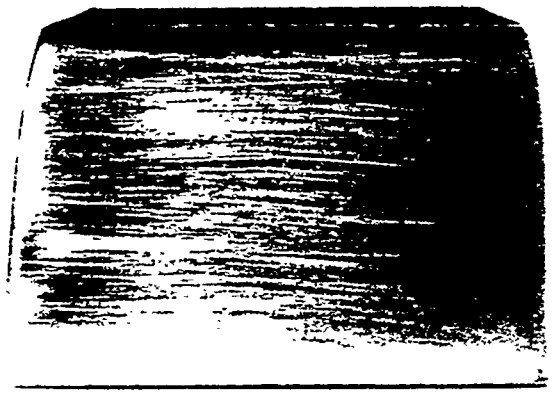

RIGHT SIDE

(2.7X)

FIGURE 39. CROSS SECTION OF SAMPLE IN FIGURE 38.

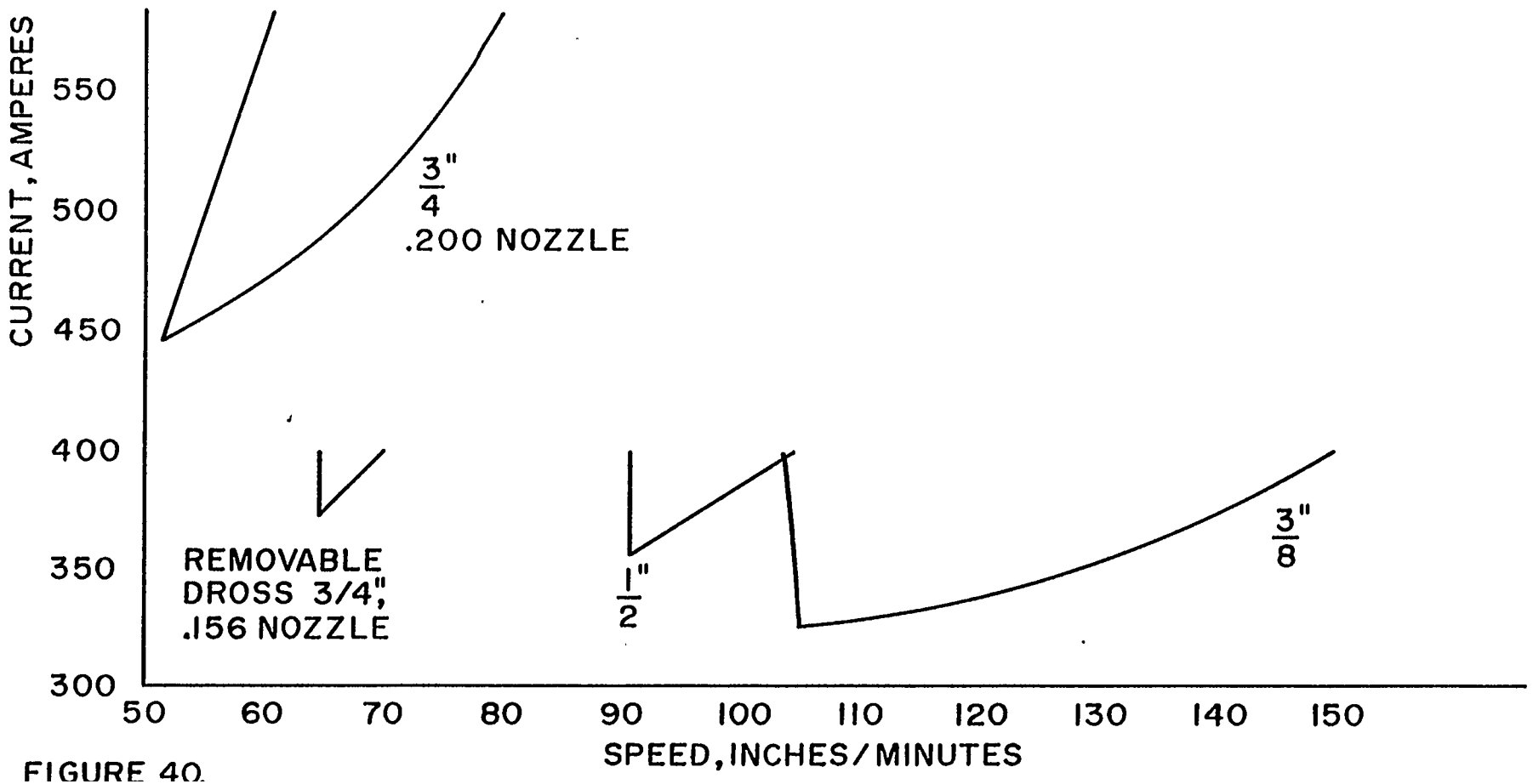
1022 STEEL
PT-15
STANDARD CONDITIONS
CURRENT, AMPERES
550
500
450
400
350
300
3/4"
.200 NOZZLE
REMOVABLE
DROSS 3/4",
.156 NOZZLE
1/2"
3/8"
50
60
70
80
90
100
110
120
130
140
150
SPEED, INCHES/MINUTES

FIGURE 40.

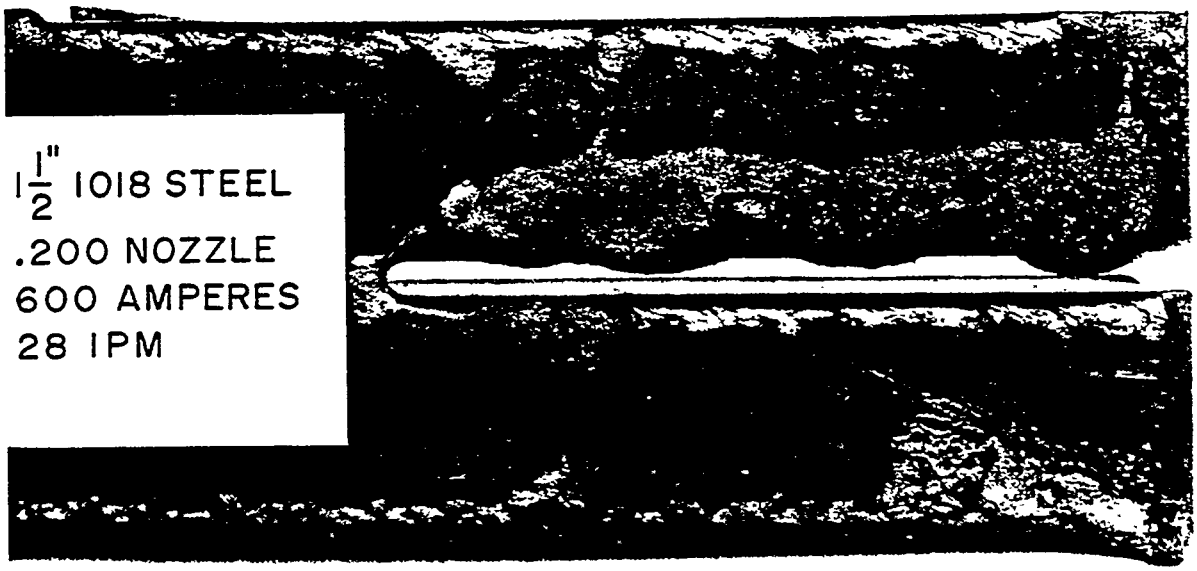

(1.2X)

FIGURE 41.

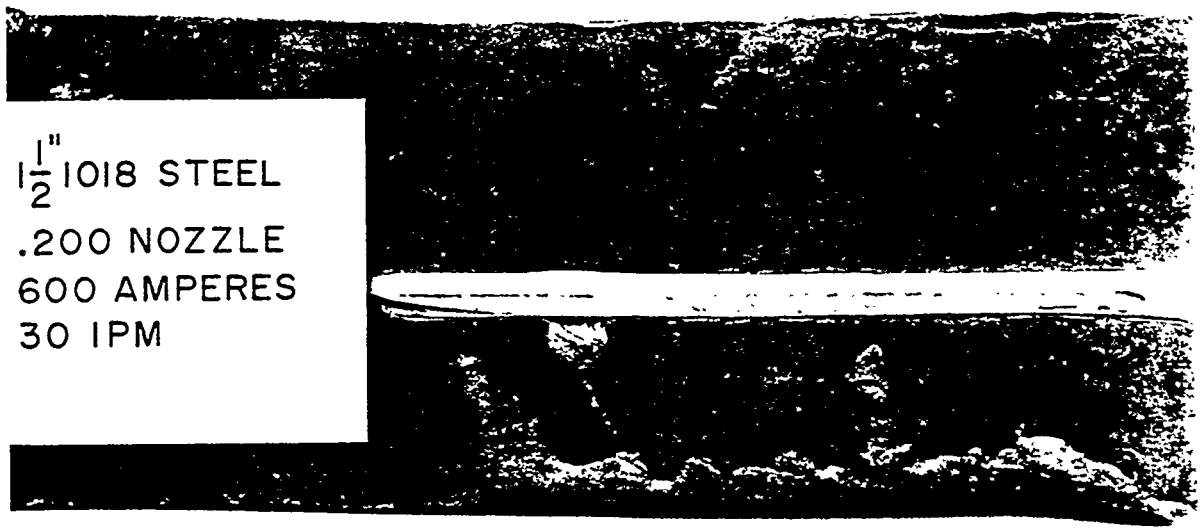

(1.2X)

FIGURE 42.

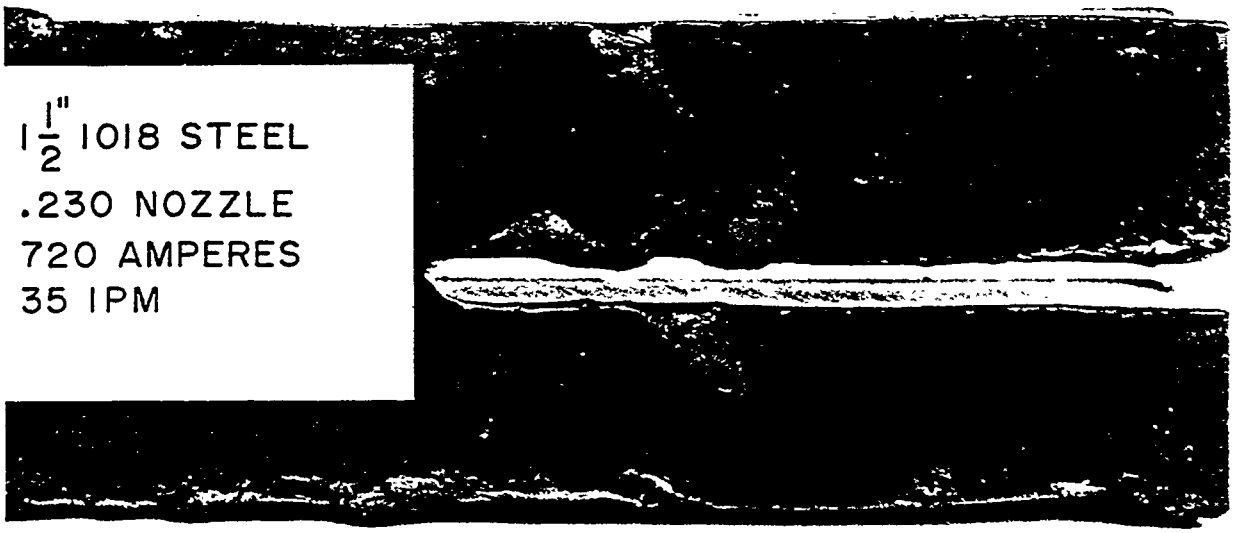

(1.2X)

FIGURE 43.

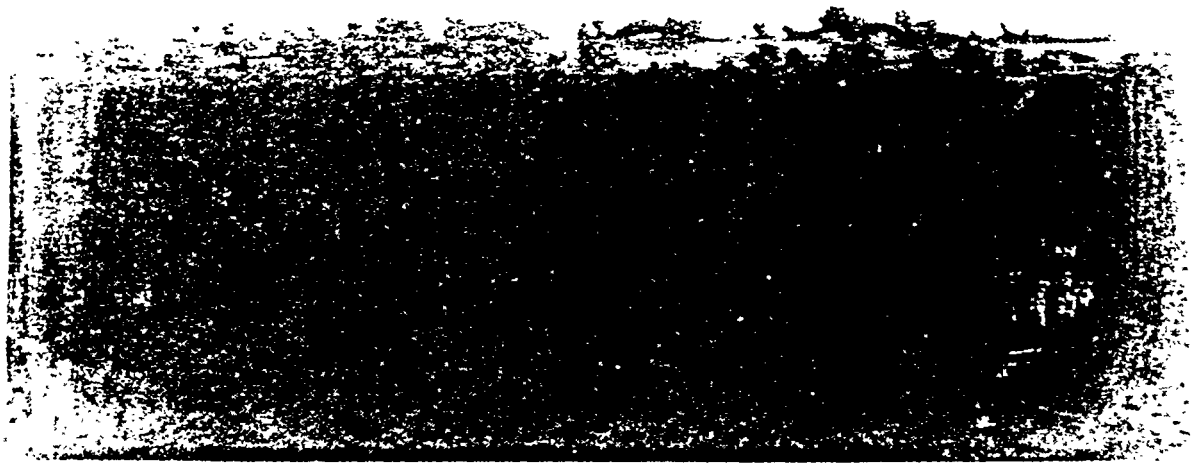

(IX)

FIGURE 44. 2" STAINLESS STEEL, CONVENTIONAL CUT, GAS: ARGON-HYDROGEN (H-30), CURRENT: 280 AMPS ORIFICE DIA: .080", SPEED: 12 IPM.

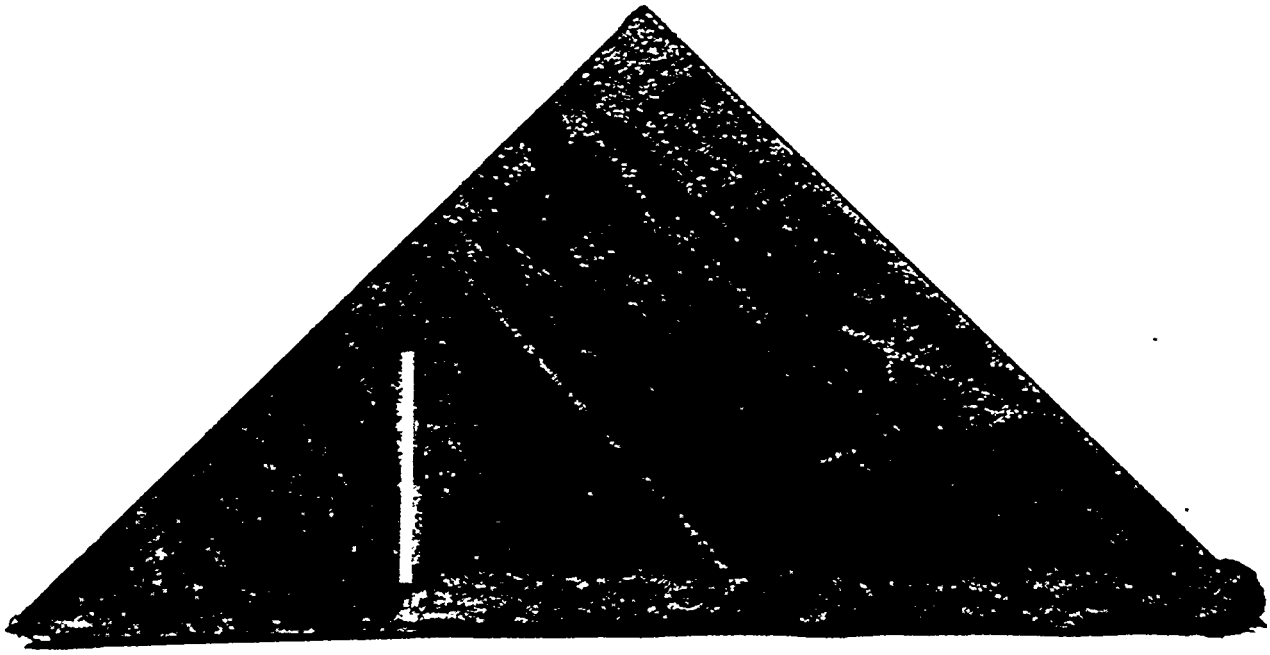

(0.8X

FIGURE 45. $\frac{3}{4}$" 1018 STEEL, BOTTOM VIEW. SCALE REMOVED FROM TOP SURFACE ON LEFT OF LINE.

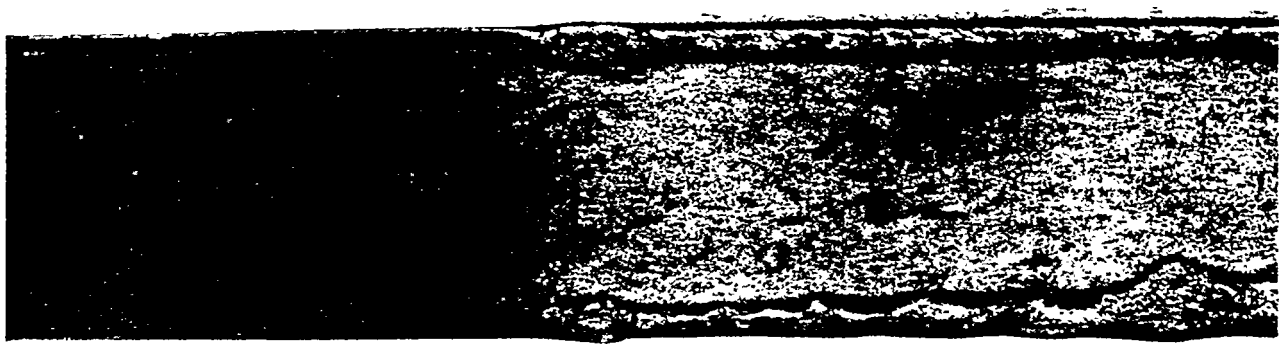

(1.3X

FIGURE 46. — SHIP STEEL, IRON-OXIDE PRIMER ON LEFT HALF.

(1.2X)

FIGURE 47. $\frac{3}{4}$" ABS PLATE, ZINC PRIMER REMOVED FROM RIGHT HALF.

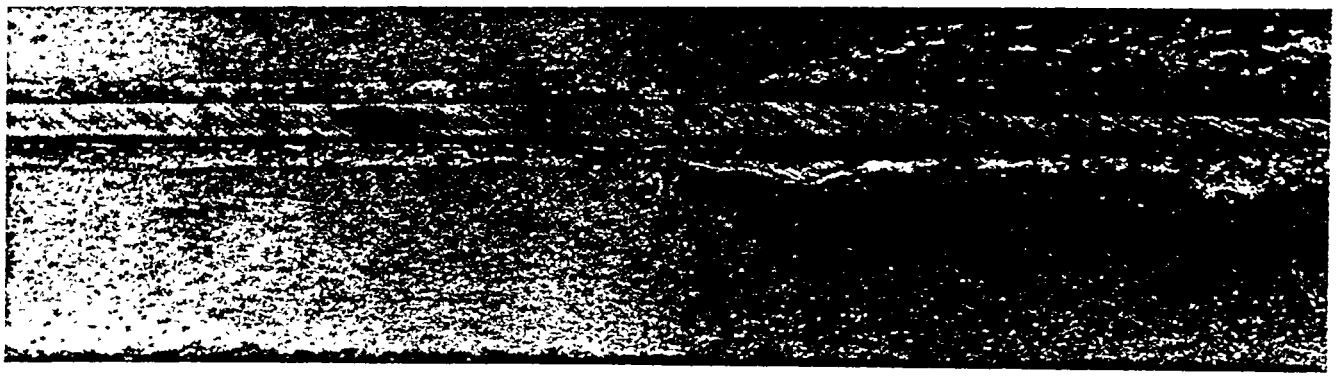

(1.2X)

FIGURE 48. $\frac{3}{4}$" SANDBLASTED ABS PLATE, ZINC PRIMER ADDED ON LEFT HALF.

(1.2X)

FIGURE 49. $\frac{3}{4}$" SCALY ABS PLATE. ZINC PRIMER ADDED ON RIGHT HALF.

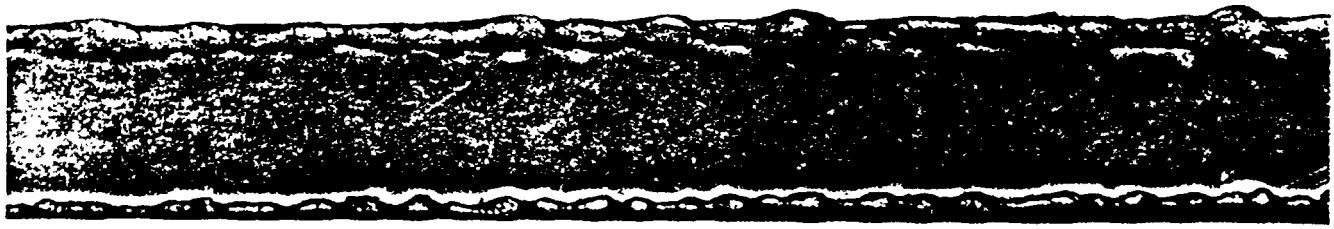

(1.2X)

FIGURE 50. $\frac{3}{4}$" PRIMED ABS PLATE, 400 AMPS, 20 IPM.

(1.2X)

FIGURE 51. $\frac{3}{4}$" PRIMED ABS PLATE, 400 AMPS, 50 IPM.

(1.2X)

FIGURE 52. $\frac{3}{4}$" PRIMED ABS PLATE, 400 AMPS, 70 IPM.

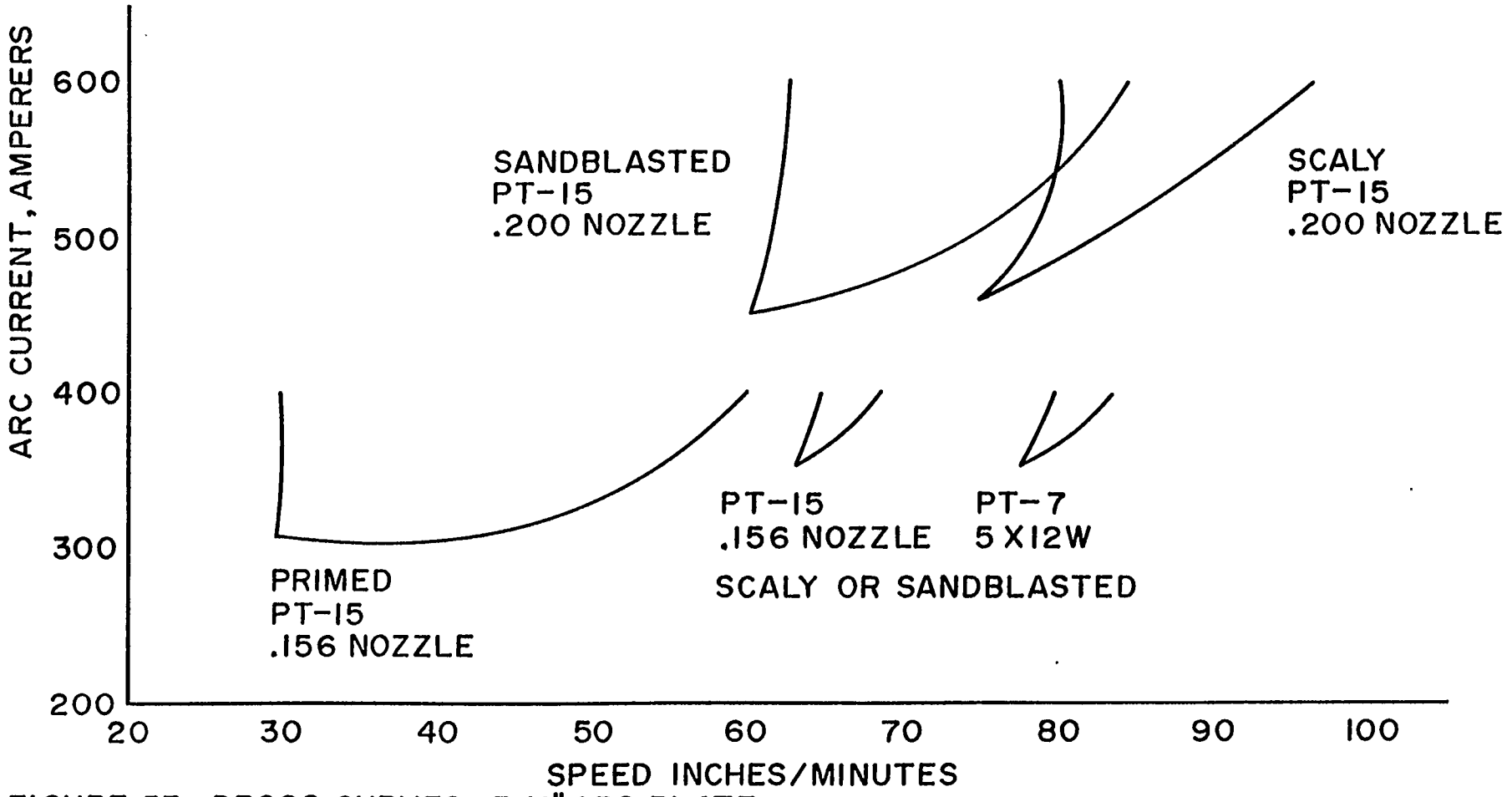

FIGURE 53. DROSS CURVES, 3/4" ABS PLATE.

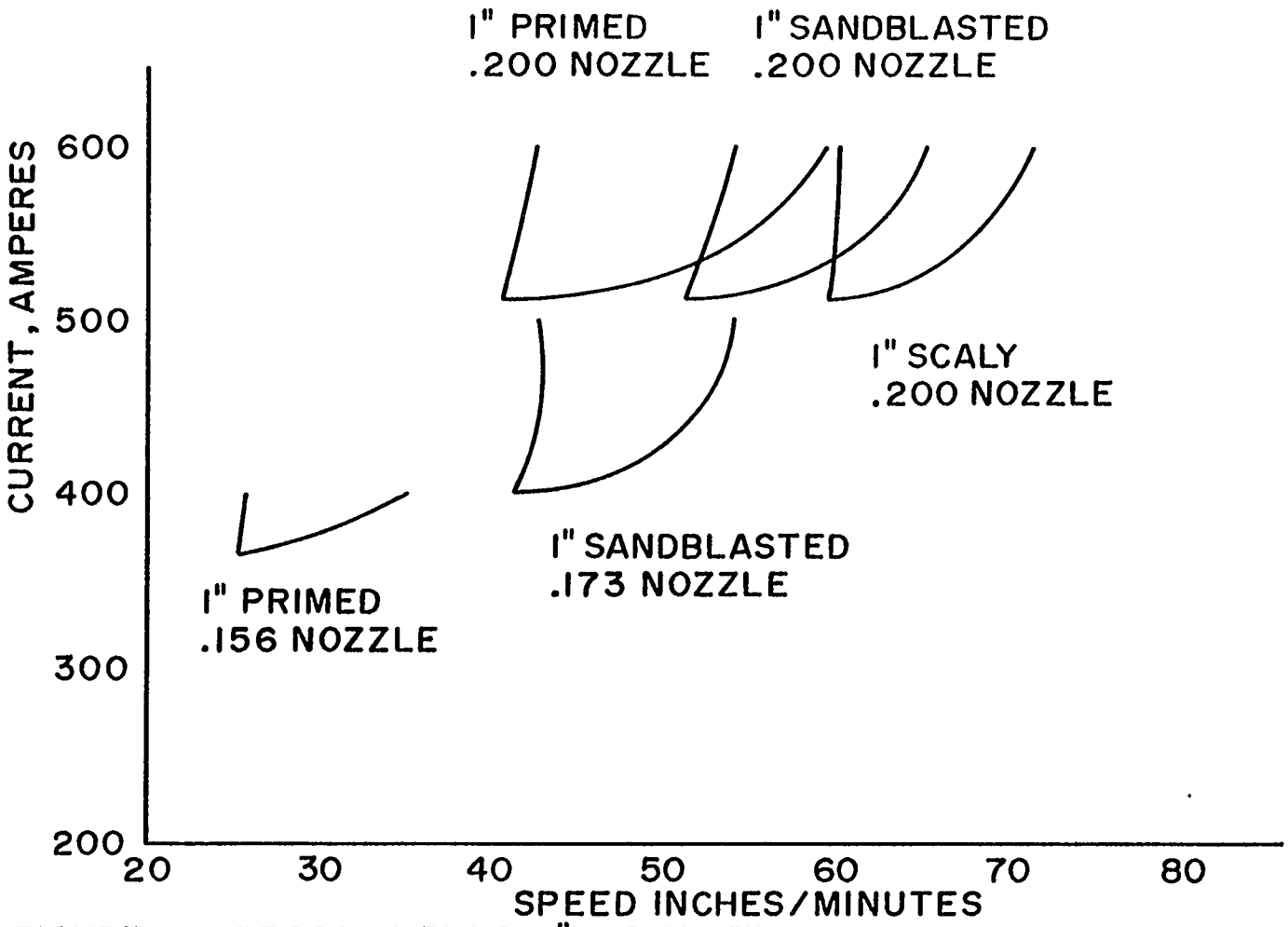

FIGURE 54. DROSS CURVES, 1"ABS PLATE.

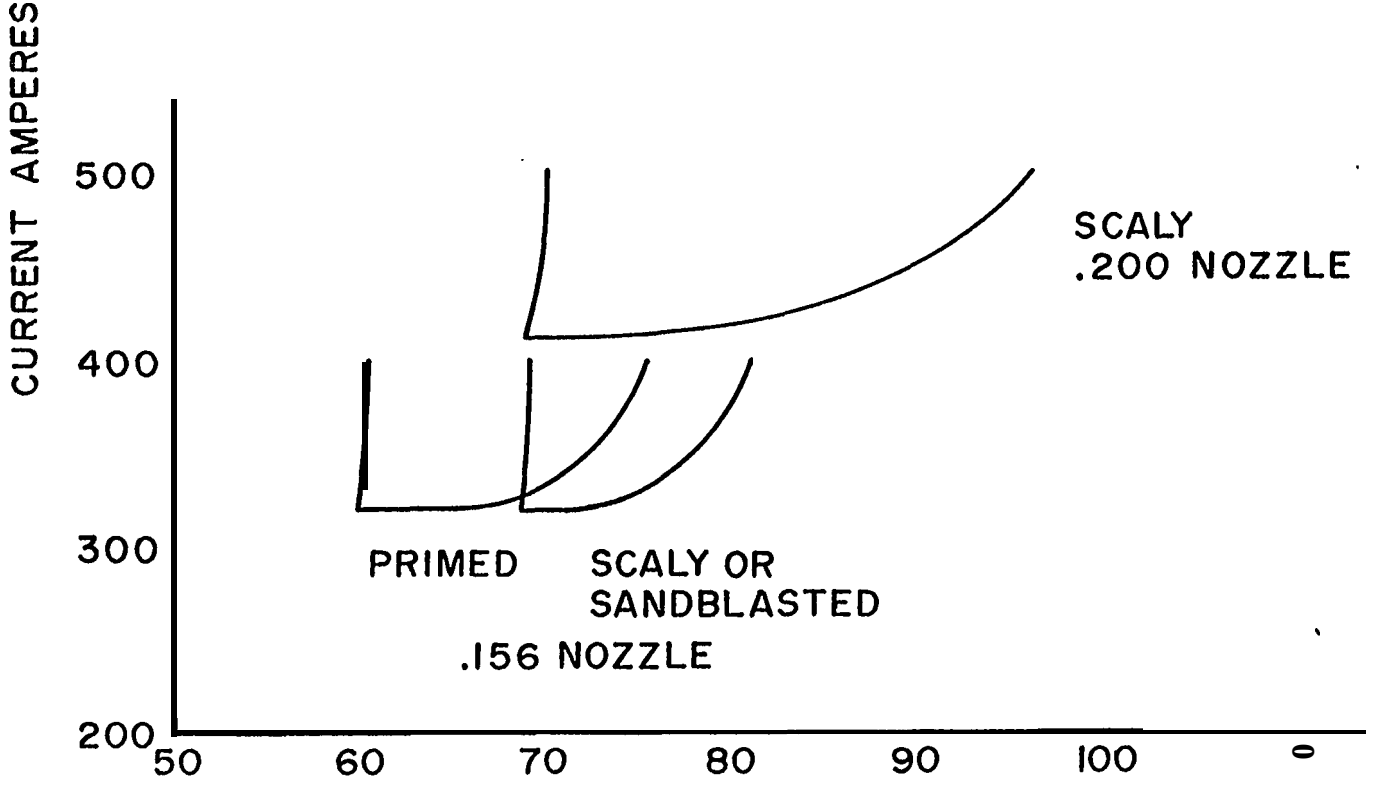

FIGURE 55. DROSS CURVES, 5/8" ABS PLATE.

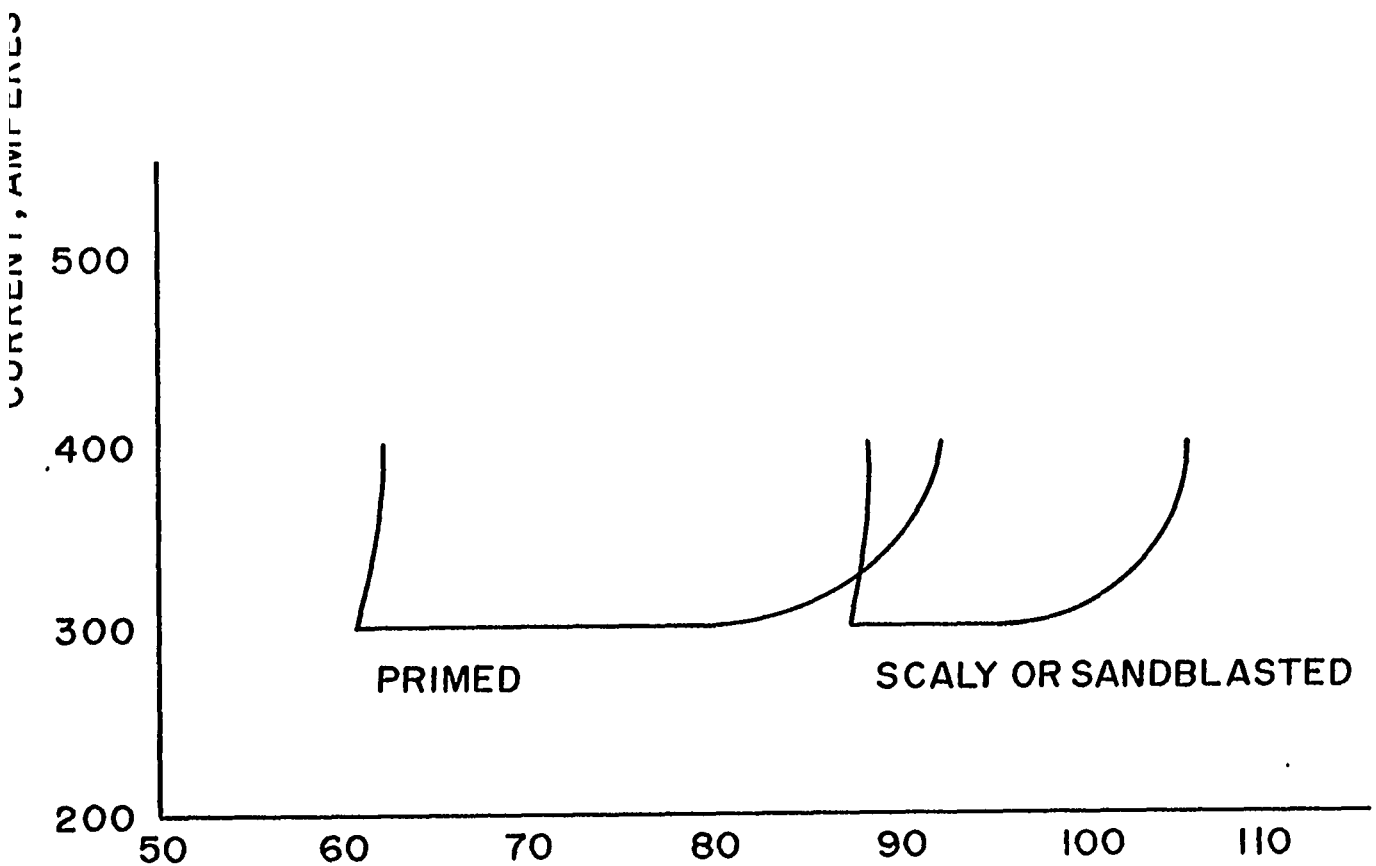

FIGURE 56. DROSS CURVES, 1/2"ABS PLATE.

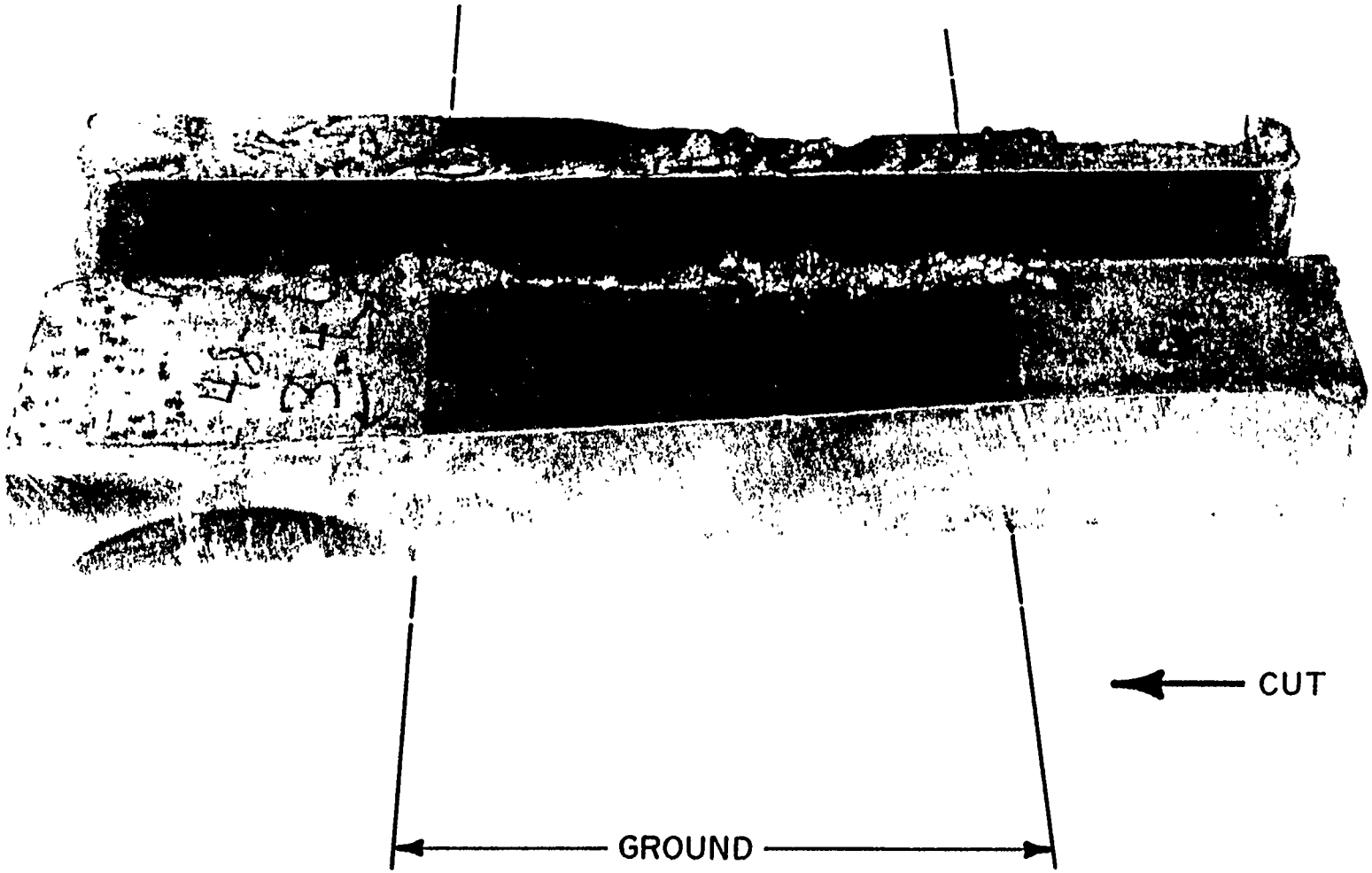

FIGURE 57. $\frac{3}{4}$" SANDBLASTED ABS PLATE, SMOOTH SURFACE IN MIDDLE.